SVU-International Journal of Engineering Sciences and Applications (2025) 6(2): 104-129
Print ISSN 2785-9967 | Online ISSN 2735-4571
DOI 10.21608/SVUSRC.2025.385645.1286

Optimization-Based Metaheuristic Techniques for Sizing and Managing Uncertainty in Hybrid Renewable Energy Systems Considering Demand-Side Challenge

Mohamed Hassanein [1], Mohamed A. Mohamed [1,□], Ahmed Hassan [1]

Abstract— Providing electricity to remote areas is more expensive and technically challenging than in grid-connected areas. Meanwhile, the effects of climate change have been exacerbated by overreliance on fossil fuels such as coal, oil, and natural gas used for power generation, transportation, and industry, leading to high CO_2 emissions and environmental degradation. In response to fuel depletion and energy crises, researchers have turned to clean, renewable alternatives including wind, Photovoltaic (PV), geothermal, hydropower, and green hydrogen. Despite their sustainability, the intermittent nature of renewable resources raises concerns about energy reliability, especially in off-grid applications. To address this problem, Integrated Hybrid Renewable Energy Systems (IHRES) combine multiple renewable sources with storage solutions such as batteries, supercapacitors, and fuel cells in addition to a backup Diesel Generator (DG). This paper presents a techno-economic analysis of a standalone PV/wind/DG/battery system for New Minya, Egypt, using real-time meteorological data. Advanced metaheuristic algorithms, along with Demand Side Management (DSM), Load Following (LF), and Cycle Charging (CC) strategies, are applied to optimize system sizing and minimize the Cost of Energy (COE), while meeting constraints such as Loss of Power Supply Probability (LPSP) and dummy energy. Among eight tested optimization algorithms, the Salp Swarm Algorithm (SSA) demonstrated the best performance, delivering the most reliable and cost-effective microgrid configuration.

Keywords:. Microgrids; Demand Side Management (DSM); Cost of Energy (COE); Renewable Energy; Loss of Power Supply Probability (LPSP); Uncertainty; Optimization.

Received: 15 May 2025/ Accepted: 3 September 2025
□ Mohamed A. Mohamed, dr.mohamed.abdelaziz@mu.edu.eg,
1. Electrical Engineering Department, Faculty of Engineering, Minia University, Minia 61519, Egypt

1 Introduction

1.1 Motivation and persuasion

To promote a clean, sustainable, and well-developed environment powered by Renewable Energy (RE), many countries have turned to developing remote areas by establishing new residential cities to accommodate growing populations [1,2]. Extensive planning and feasibility studies have been conducted to explore the electrification of these areas through grid extension. However, results have shown that connecting these remote regions to the national grid is prohibitively expensive and, in some cases, technically constrained [3-7].

Additionally, continued dependence on fossil fuels-such as diesel, natural gas, coal, mazut, and oil for power generation, transportation, and industrial use, contributes significantly to climate change [8,9]. These resources are finite and cause environmental degradation due to the emission of Greenhouse Gases (GHGs), especially Carbon Dioxide (CO_2) [10-12].

In response, many countries are increasingly turning to clean, renewable, and environmentally friendly energy sources-such as Photovoltaic (PV) energy, wind energy, bioenergy, Heat Pump Technologies (HPT), geothermal, tidal, Green Hydrogen (GH), Hydropower (HP), and ocean energy as sustainable alternatives to fossil fuels [13,14].

The International Energy Agency (IEA) projects that almost 3700 GW of new renewable capacity will be installed worldwide between 2023 and 2028. By 2028, renewables are projected to supply over 42% of the world's electricity, with PV and wind energy experiencing annual growth rates of 9.5% and 6.1%, respectively, between 2020 and 2028 [15]. In Egypt, PV and wind are among the most promising renewable energy sources.

Despite their potential, the intermittent nature of solar radiation and wind speed remains a significant obstacle [16], making it difficult to depend mainly on these sources to power microgrids. While connecting RE microgrids to the

national grid in a two-way power flow configuration can help stabilize supply [17-19], such integration is often financially and technically impractical in isolated regions [20-22].

As a viable alternative, hybrid systems that integrate various renewable and conventional energy sources, along with energy storage technologies such as batteries, Fuel Cells (FC), supercapacitors, Flywheels (FWs), molten salt, hydroelectric pumped storage (HPSS), and compressed air can offer more reliable and cost-effective solutions. Incorporating a standby Diesel Generator (DG) further enhances system reliability [23,24].

This study aims to determine the optimal sizing of components for an isolated hybrid energy system consisting of PV cells, Wind Turbines (WT), DGs, and batteries for New Minya City in Egypt. The system is designed using real-time meteorological data, such as global horizontal irradiation (GHI) and wind speed recorded at 50 meters.

1.2 Literature review on optimization techniques and sizing methods

Several studies have explored the techno-economic sizing of standalone hybrid renewable energy systems (HRES), particularly for applications in remote areas. These studies present various system configurations, with the most common combinations involving solar PV and wind energy, often supported by battery storage or diesel generators for backup power [25-27]. Alternative configurations utilize other renewable sources [28,29], with excess energy stored in different types of storage technologies [30,31]. Overall, sizing approaches for HRES can be grouped into three primary categories:

1.2.1 Sizing hybrid energy systems with software tools

Several commercial software tools, primarily developed in C++ for Windows platforms, are widely used for hybrid energy system sizing and analysis:

RETScreen (Canada, 1998) supports energy system sizing with technical, financial, and environmental evaluations, including system losses and cogeneration. The latest version is a multi-agent tool designed to optimize PV systems, WT, DG, and battery storage, achieving more than a 99% reduction in greenhouse gas emissions through the use of renewable energy sources [32,33].

iHOGA (Improved Hybrid Optimization by Genetic Algorithm) optimizes hybrid systems combining renewable and conventional resources (e.g., PV, WT, FC, hydro, batteries, DG. It reduced CO_2 emissions by 73.8% and unmet load by 68% in a Paris-based PV/WT/DG/Battery case study [34].

Hybrid2 (1996, University of Massachusetts) analyzes PV/WT/battery-based systems with high performance. It was applied in sizing a PV/WT/FC system in Chicago [35-37].

HOMER (1993, NREL) is intended for both on-grid and off-grid systems. In Shiraz, it was used to size a PV/WT/DG/Battery system, resulting in a 43.9% renewable energy contribution while reducing costs (9.3–12.6 c/kWh) and CO_2 emissions [38,39].

HybSim (1987, Sandia National Labs) simulates off-grid hybrid systems (PV, DG, batteries), offering techno-economic analysis and reliable cost predictions. It requires detailed load, weather, and economic data [40,41].

TRNSYS (1975, Universities of Wisconsin and Colorado) started as a thermal system simulator and now supports hybrid systems, including solar thermal and PV for HVAC-integrated buildings. It provides detailed thermal and electrical system analysis [42,43].

Dymola (ISE, Germany) models hybrid systems with PV, WT, DG, FC, and batteries, focusing on life cycle cost analysis [44].

1.2.2 Sizing hybrid energy systems with traditional methods

Traditional or deterministic methods are widely used for sizing hybrid energy systems. The four primary approaches include:

- Analytical Method:

This method models the hybrid energy system with numerical equations and uses system sizing as a viability function. In South Africa, it optimized photovoltaic panels and wind turbines, achieving an energy cost of 0.97 €/kWh and annual production of 100 GWh [45]. Although it is fast, the approach lacks flexibility in general optimization applications.

- Iterative Method:

This iterative algorithm optimizes the design by minimizing energy cost and maximizing reliability. Applied to a hybrid system of PV panels, wind turbines, and battery storage in Brazil, the lifecycle cost was $25,672 [46]. However, it lacks consideration of key factors like wind turbine hub height, blade rotation angle, solar panel tilt, and radiation type.

- Probabilistic Method:

This probabilistic algorithm sizes the hybrid energy system by accounting for wind speed variations and system component adjustments, affecting wind turbine power. While easy to use, it doesn't yield optimal results. For a PV/WT/biomass/battery system, it led to increased storage and component ratings, raising the total cost [47]. This

method is simple but doesn't maintain the hybrid system's dynamic performance.

- Artificial Intelligence (AI) Methods:

This advanced method controls, configures, and sizes hybrid energy system components by emulating tasks performed by the human mind [48,49], mine blast algorithm (MBA) [50], preference inspired co-evolutionary algorithm (PICEA) [51], Artificial bee swarm algorithm [52], Artificial neural network (ANN) [53], fuzzy logic [54] and Discrete Harmony Search (DHS) [55].

1.2.3 Sizing of hybrid energy system using metaheuristic algorithms

After examining several types of size techniques, we discovered that no one could consistently deliver optimal solutions for the desired multi-objective function. As a result, metaheuristic algorithms have emerged as effective techniques over the past decade [56]. These algorithms surpass traditional software and deterministic methods in sizing hybrid renewable energy systems. The most effective approach, known as hybridization, integrates renewable energy sources, including solar PV, wind turbines, biomass, biogas, and tidal energy, with conventional energy sources such as diesel generators. Below, we will review artificial algorithms used for sizing PV/WT/DG/battery systems with different objective functions:

In [57,58], Strength Pareto Evolutionary Algorithm (SPEA) optimized the size of a PV/WT/DG hybrid system, focusing on minimizing system costs and greenhouse gas emissions.

In [59-61], Genetic Algorithm (GA) optimized a PV/WT/battery system, addressing objectives like maximizing reliability, minimizing lifecycle cost, and reducing power supply loss.

In [62,63], Particle Swarm Optimization (PSO) was applied to size a PV/WT/DG/battery system under resource uncertainty. PSO was also used in [64] for a hybrid PV/WT/FC/electrolyzer/hydrogen storage system with wind uncertainty and reliability constraints.

In [65], the Simulated Annealing Algorithm (SAA) optimized a PV/WT hybrid system, minimizing lifecycle cost.

In [66], Response Surface Methodology (RSM) provided optimal sizing for a PV/WT/battery system with reduced power supply loss and fossil fuel consumption, comparing favorably to SAA.

In [67], A combination of PSO and GA optimized mathematical models for hybrid systems. A comparison in [68] showed PSO's superiority in terms of convergence, speed, and accuracy.

In [69,70], Multi-Objective PSO (MOPSO) optimized a PV/WT/FC/hydrogen system, improving energy cost, reliability, and minimizing outages, outperforming PSO.

In [71], A combination of Sequential Monte Carlo Simulation (SMCS) and Pattern Search (PS) optimized a hybrid energy system, outperforming the GA-SMCS combination.

In [72], the Cuckoo Search Algorithm (CS) optimized a PV/WT/DG/battery system, providing more accurate results than GA and PSO.

In [73], the Multi-Objective Self-Adaptive Differential Evolution (MOSADE) algorithm optimized a PV/WT/DG/battery system, reducing processing time.

In [74], the Artificial Bee Colony (ABC) algorithm optimized a PV/WT/battery system for energy cost and reliability.

In [75], the Improved Arithmetic Optimization Algorithm (IAOA) optimized PV/WT/DG/battery and PV/DG/battery systems, minimizing total costs.

In [76], Whale Optimization (WOA), Water Cycle Algorithm (WCA), and Moth-Flame Optimizer (MFO) were used for a PV/WT/DG/battery system, minimizing lifecycle costs while enhancing reliability and efficiency.

1.3 Energy saving and reliability concepts

In microgrids, the discrepancy between load demand and the available generation from different energy sources leads to higher energy costs. This is due to the need for extensive generation and distribution network expansions to meet load demands, often forcing energy sources to operate beyond their rated capacity during peak periods [77].

Balancing load and generation is required to reduce these costs and avoid expensive installations [78]. Additionally, load demand curves should be flexible to reduce the burden on power generation equipment, ensure proper functioning of protective components, and minimize energy costs while preserving capacity for future expansion. In the first section, we will explore Demand Side Management (DSM) strategies.

System reliability, which reflects its strength, depends on the nature of energy sources and their response to internal faults or intermittent renewable sources like wind and solar. In the second section, we will discuss the concept of uncertainty, which is vital for determining optimal sizing.

1.3.1 Demand side management Strategy

DSM aims to match load demand with available generation to manage peak load periods. It includes methods like “peak clipping, valley filling, load shifting, energy conservation, load building, and flexible load shape” [79], as shown in **Fig. 1** and explained below [80]:

Peak clipping: It is used when the microgrid capacity cannot meet peak load demand. This is done by turning off appliances or encouraging demand changes through higher energy prices during peak hours.

Load Growth: This strategy aims to increase load when generation exceeds demand, helping maintain system stability, improve load-sharing, and enhance grid flexibility. It can be achieved by increasing electricity tariffs.

Energy Efficiency: It is commonly called energy-saving. This strategy reduces energy demand by using efficient devices, switching off non-essential loads, or raising electricity tariffs, thus lowering load demand, and reshaping the load profile.

Flexible Load Shape: It is also known as dynamic load management; this strategy adjusts the load based on available generation. It can be achieved by implementing dynamic electricity tariffs that fluctuate in price.

Load shifting: Low-priority loads move from peak to off-peak hours without altering the total energy consumption. For example, customers can store thermal heat or move tasks like laundry to off-peak times, improving load factor and avoiding peak periods. This is enabled by higher prices during peak hours and lower prices during off-peak hours.

Valley filling: It aims to increase loads during off-peak hours when generation exceeds demand, enhancing average energy utilization. This is achieved by activating low priority loads or incentivizing customers to use energy during these times with reduced energy prices.

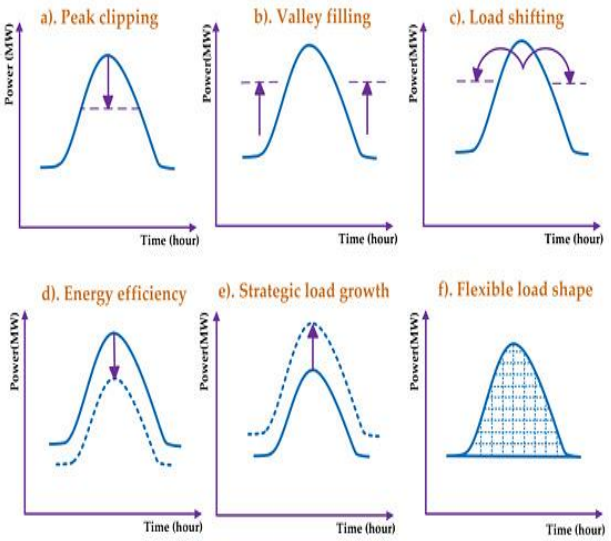

Fig. 1 Demand-side management strategies.

1.3.2 Uncertainty analysis

The intermittent nature of solar and wind energy creates uncertainty in Hybrid Renewable Energy Systems (HRES), presenting challenges for stand-alone systems' operation and performance in addition to their design [81-84]. Load consumption also contributes to this uncertainty. Effective long-term planning and real-time operation of microgrids depend on ensuring energy balance while maintaining sufficient reserves. Additionally, capital, operation, and maintenance costs are important factors in microgrid design and planning [85,86].

To address uncertainties, microgrid designers incorporate reliable technologies such as backup diesel generators, energy storage systems (e.g., batteries and supercapacitors), demand-side management, and vehicle-to-grid strategies. Properly accounting for these uncertainties during the planning stage helps system operators maintain power balance at the lowest cost, as operational flexibility may be limited.

1.4 Contribution and paper organization

Unlike many earlier studies that primarily aimed to minimize annual costs, this work adopts a more comprehensive approach by incorporating DSM, CC, LF and various uncertainties. Advanced metaheuristic optimization techniques are employed to improve the resilience and operational reliability of an isolated-grid RE system comprising PV panels, WT, DG, and battery storage. Moreover, this study stands out by examining system performance under fluctuating demand profiles and the inherent variability of renewable resources. The main contributions of this paper are as follows:

1. Comprehensive system analysis using high-performance metaheuristic algorithms to design an integrated RE system, demonstrating superior performance over commercial software and conventional methods. A detailed comparative evaluation of the applied techniques is presented.
2. Development of a multi-objective optimization framework for sizing hybrid PV/WT/DG/battery systems. This framework minimizes COE, LPSP, and excess (dummy) energy, while maximizing system reliability and operational performance.
3. A strategic methodology for achieving maximum power output and minimum energy cost in Hybrid Renewable Energy Systems (HRES).
4. Integration of DSM, CC, and LF strategies to efficiently meet demand requirements while reducing component sizing and overall lifecycle costs.
5. Utilization of solar radiation and wind speed datasets specific to New Minya, Egypt, derived from NASA and 20 years of historical meteorological records.
6. To the best of the authors' knowledge, this is the first study to optimize HRES component sizing in a remote area using real-time and location-specific meteorological data.

2 Development of an IHRES

The following stages explain a systematic approach that is necessary to implement an IHRES for isolated communities:

2.1. Identification of Study Area

New Minya City, located in the Minya Governorate of Egypt, has been selected as the study area. It lies on the eastern bank of the Nile River, directly opposite Old Minya. The geographical location of New Minya within Egypt is shown in **Fig. 2** It is located at a height of 123 meters above mean sea level, in latitude 28.0986° N and longitude 30.8327° E. The city is 24.6 thousand acres in total, of which 6.5 thousand acres are built (residential areas, services, industry, tourist, and leisure, etc.). The utilities and infrastructure sector maintains four sanitation pumping plants with a daily capacity of 9.6 thousand. Additionally, the industry sector includes 59 factories that are currently in production and 68 factories that are under construction. The number of service buildings implemented by New Urban Communities' Authorities (NUCA) is about 74 [3] as follows:

- 19 educational buildings
- 10 hospitals and centers
- 11 commercial services
- 6 nurseries
- 5 mosques
- 9 social services
- 11 public services
- 1 communication center
- 11 buildings by NUCA
- 84 buildings by the private

2.2. Visualization of Electrical Demand

This study focuses on supplying electricity to the utilities and infrastructure sector of New Minya city, covering the residential, commercial, and industrial sectors across 6 districts, club areas, build-your-own-house zones, roads, communications, and extended networks. It also includes a drinking water plant, a sanitation plant with 4 pumping stations, and the cultivation of green spaces and forestation. **Figure 3** illustrates the hourly power demand profile over one year. The average load is approximately 22,500 kW, with a peak demand of 42,000 kW and a minimum load of 7,000 kW.

Fig. 2 The geographical location of New Minya City

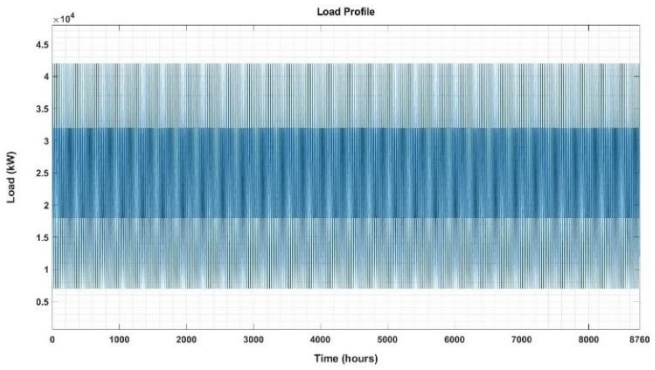

Fig. 3 Hourly load power for New Minya city

2.3 Assessment of natural resources

Based on meteorological data, the mean annual wind speed in New Minya city is approximately 5.19 m/s at a height of 10 meters (the level of the anemometer suspension), as illustrated in **Fig. 4**.

Meteorological data shows the annual average solar energy curve for the selected site. **Figure 5** depicts the 24-year average (1994-2018) used in the simulation, approximately 6.05 kWh/m²/day.

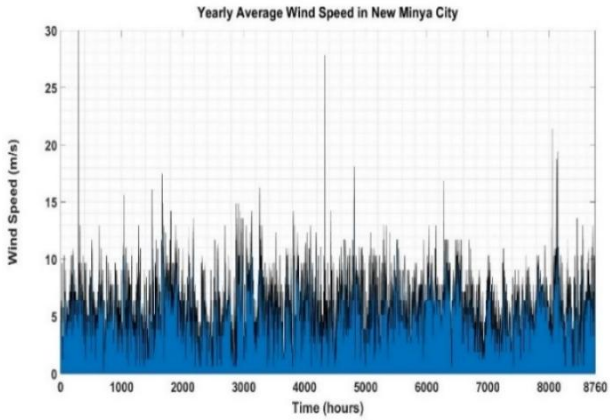

Fig. 4 The yearly average wind speed in New Minya city

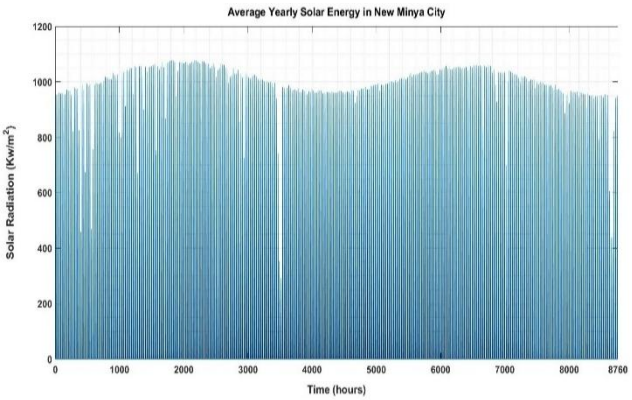

Fig. 5 The average yearly solar energy for New Minya City

The annual average ambient temperature curve from meteorological data is shown in **Fig. 6**. The simulation considered a 24-year average (1994–2018) with a mean temperature of 25.58ºC (78.04ºF).

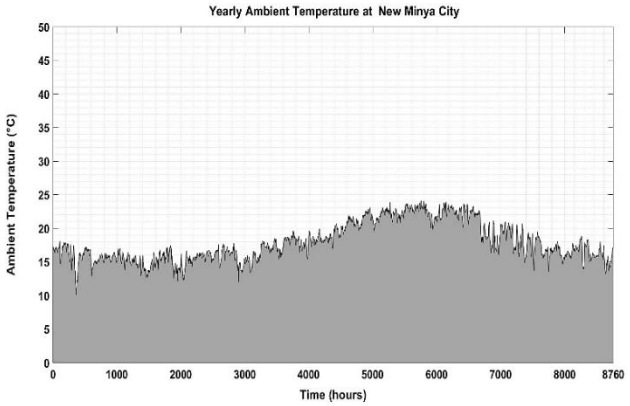

Fig. 6 The hourly ambient temperature at the New Minya site

3 Mathematical Modelling of the IHRES Components

An accurate mathematical model of each component is essential to determine the optimal sizing of the Integrated Hybrid Renewable Energy System (IHRES). The proposed system includes solar PV modules, wind turbines (WTs), a diesel generator (DG) as a backup power source, and a battery bank. This configuration is particularly suitable for addressing electricity shortages in New Minya, Egypt. The IHRES architecture, shown in **Fig. 7**, consists of seven main components: solar PV modules, wind turbines, a diesel generator, a battery bank, a bidirectional power converter, a dump load, and the service load.

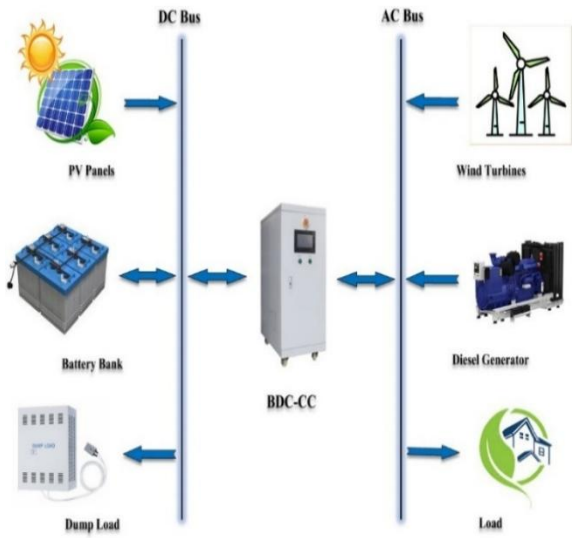

Fig. 7 The IHRES's configuration

3.1 Solar Energy System Model

Various models for calculating PV output power are available in the literature. In this study, $\boldsymbol{P_{PV}(t)}$ is estimated using a simplified model based on hourly solar $\mathbf{G(t)}$ [87] as in (1).

$$P_{\mathrm{PV}}(\mathrm{t}) = N_{\mathrm{PV}} * PV_{\mathrm{panel\_rating}} * \left(\frac{\mathrm{G(t)}}{G_{\mathrm{ref}}}\right) * [1 + K_{\mathrm{T}} * (T_{\mathrm{C}} - T_{\mathrm{ref}})] \quad (1)$$

Where $PV_{\mathrm{panel\_rating}}$ is the rated power of the PV panel, N_{PV} is the number of PV panels, G_{ref} is the reference solar radiation (1000 W/m²), K_{T} is the temperature coefficient (3.7×10^{-3} 1/°C), T_{C} represents the average annual temperature (°C), and T_{ref} is the PV cell temperature under Standard Test Conditions (STC) at 25°C. The average annual temperature of the cell can be calculated as in (2).

$$T_C(t) = T_{amb} + [0.0256 * G(t)] \quad (2)$$

Where T_{amb} is the ambient temperature (°C) for the selected PV module. The energy generated $E_{\mathrm{PV}}(\mathrm{t})$ from PV panels is calculated as in (3) [87,88].

$$E_{\mathrm{PV}}(\mathrm{t}) = P_{\mathrm{PV}}(\mathrm{t}) * \Delta t \quad (3)$$

Where Δt denotes the time interval, corresponding to one hour.

3.2 Wind Energy System Model

Wind resources and a Wind Turbine's (WT) energy generation capacity at a location depend on hub height wind speed, WT speed characteristics, and land surface type. The wind speed at the desired hub height, relative to the anemometer height, can be calculated as in (4) [88].

$$u(h) = u(h_a)\left(\frac{h}{h_a}\right)^{\alpha} \quad (4)$$

Where u(h) represents the wind speed at hub height (m/s), u(h_a) is the measured wind speed (m/s), and α\alpha is the site-specific roughness factor. IEC standards [89] specify a friction coefficient of 0.20 for normal winds and 0.11 for strong winds, with a value of (1/7) used in this paper.

The formula for estimating the WT's mechanical power to the turbine is as in (5).

$$P_{mech} = \frac{1}{2}\rho A C_p u^3 \quad (5)$$

Where A is the rotor swept area (m²), u is the wind speed (m/s), C_p is the power coefficient, and ρ\rho is air density (kg/m³). The power coefficient C_p, or Betz's coefficient, is a function of the rotor tip-speed to wind speed ratio (λ \lambda), with a theoretical maximum of 0.593 [90].

$$\lambda = \frac{\omega R}{u} \quad (6)$$

Where R is the radius of the wind turbine (m), and ω (omega) is the angular velocity (rad/s).

The power output at a constant wind speed is illustrated in **Fig. 8**.

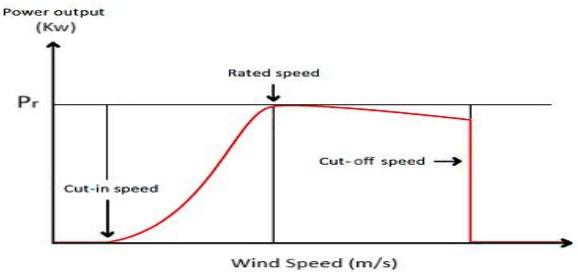

Fig. 8 Wind turbine power characteristics

The *cut-in speed* refers to the minimum wind speed at which a wind turbine begins generating electricity, while the *cut-off speed* is the maximum wind speed at which the turbine is shut down to prevent mechanical stress or damage. The *rated power output* is achieved within the range between these two thresholds, during which the turbine operates at its maximum capacity.

Using the WT's normal power curve parameters, the estimated power P_{WT} is given as in (7) [91, 92].

$$P_{WT} = 0 \tag{7.1}$$

$$P_{WT} = \frac{N_{WT} * \eta_{WT} * P_{R_{WT}} * (u^2(t) - u^2{}_{cut-in})}{u^2{}_{rated} - u^2{}_{cut-in}} \tag{7.2}$$

$$P_{WT} = N_{WT} * \eta_{WT} * P_{R_{WT}} \tag{7.3}$$

(7.1) IF $u(t) < u_{cut-in}$ OR $u(t) > u_{cut-off}$

(7.2) IF $u_{cut-in} \le u(t) \le u_{rated}$

(7.3) IF $u_{rated} < u(t) \le u_{cut-off}$

Where N_{WT} is the number of WTs, u_{cut-in} is the cut-in speed(m/s), u_{rated} is the rated speed(m/s), $u_{cut-off}$is the cut-off speed(m/s), and P_{R_WT} is the rated output power(kW).

The wind energy capacity at a location can be estimated using the Weibull distribution to analyze wind speed data. Various methods exist for calculating the Weibull parameters k and c. The probability density function for wind speed (u) in a two-parameter distribution is as in (8) [93].

$$f(u) = \frac{k}{c} * \left(\frac{k}{c}\right)^{k-1} * exp\left[-\left(\frac{u}{c}\right)^{k}\right] \quad where, (k>0, u>0, c>0) \tag{8}$$

Where k is the shape parameter and c is the scale parameter, the cumulative distribution function (u) can be determined using (9).

$$F(u) = 1 - exp\left[-\left(\frac{u}{c}\right)^{k}\right] \tag{9}$$

The following formulas are the Weibull parameters' final results:

$$k = a \quad and \quad c = \left(-\frac{b}{k}\right) \tag{10}$$

Where parameters a and b can be estimated, respectively, as follows [88]:

$$a = \left(\sum_{i=1}^{w}(x_i - \bar{x}) * \sum_{i=1}^{w}(y_i - \bar{y})\right) / \left(\sum_{i=1}^{w}(x_i - \bar{x})^2\right) \tag{11}$$

$$b = \bar{y}_i - a x_i = \left(\frac{1}{w}\sum_{i=1}^{w} y_i - \frac{a}{w}\sum_{i=1}^{w} x_i\right) \tag{12}$$

$$y_i = ln\left(-ln\left(1 - F(u_i)\right)\right) \quad and \quad x_i = \ln(u_i) \tag{13}$$

Where w is the number of non-zero wind speeds, u_i is the wind speed (m/s) at time step i, and x_i and y_i's average values are $\bar{x}$ and $\bar{y}$, respectively.

This formula calculates the capacity factor (C_F) at a specific location as follows [90]:

$$C_F = \frac{exp\left[-\left(\frac{u_{cut-in}}{c}\right)^{k}\right] - exp\left[-\left(\frac{u_{rated}}{c}\right)^{k}\right]}{\left(\frac{u_{rated}}{c}\right)^{k} - \left(\frac{u_{cut-in}}{c}\right)^{k}} - exp\left[-\left(\frac{u_{cut-off}}{c}\right)^{k}\right] \tag{14}$$

The energy produced from WT panels (E_{WT}) is calculated as follows:

$$E_{WT}(t) = C_F * P_{WT}(t) * \Delta t \tag{15}$$

Where Δt represents the time interval and is equivalent to one hour.

3.3 Battery Storage System Model

The battery bank provides power during periods of high load demand or when renewable energy resources are unavailable, while also storing surplus energy generated. The stored energy at hour ' $t+1$' is given by the following formulae [87, 94]:

$$E_{\text{Bat}}(t+1) = (1 - \sigma) * E_{\text{Bat}}(t) + \left(P_{\text{Gen}}(t) - \frac{P_{Load}(t)}{\eta_{Conv}}\right) * \Delta t * \eta_{CC} * \eta_{BC} \tag{16}$$

When RE resources can't meet the load during discharge, the battery bank covers the shortfall, as follows [93]:

$$E_{\text{Bat}}(t+1) = (1 - \sigma) * E_{\text{Bat}}(t) - \left(\left(\frac{P_{Load}(t)}{\eta_{Conv}} - P_{\text{Gen}}(t)\right) / \eta_{BD}\right) * \Delta t \tag{17}$$

Where $P_{Load}(t)$ represents the hourly electrical demand at timeΔt, $P_{\text{Gen}}(t)$ is the generated power, and σ is the self-discharge rate (0.2%/day) [59]. Charging and discharging efficiencies (η_{BC} , η_{BD}) are 90% and 85% [95], and converter efficiency (η_{Conv}) is 95% [96].The amount of power produced by the RE resources, $P_{Gen}(t)$ is calculated as in (18).

$$P_{Gen}(t) = [P_{PV}(t) + P_{WT}(t)] * \eta_{Conv} \tag{18}$$

3.4 Diesel Generator Backup System Model

DGs support isolated grids when RE sources are insufficient or fail to meet the demand, or low battery levels. Hourly fuel consumption (F_{DG}) is calculated using a linear relationship based on the load demand [87].

$$F_{DG}(t) = [a_{DG} * P_{DG\_Gen}(t) + b_{DG} * P_{DG\_rating}] \ (l/h) \quad (19)$$

Where a_{DG} = 0.246 (l/kWh) and b_{DG} = 0.08145 (l/kWh) define the DG fuel curve [58, 97]. P_{DG_rating} is the rated power, and $P_{DG_Gen}(t)$is the hourly generated power. The following formula is used to determine the Diesel Generator's (DG) Annual Fuel Consumption (AFC):

$$AFC = \sum_{t=1}^{8760} F_{DG}(t) \quad (20)$$

3.4.1 CO_2 Emissions

According to estimates, DG's hourly fuel usage and CO_2 emissions may be estimated as follows [98]:

$$CO_2(t) = SE_{CO_2}(kg/l) * F_{DG}(t) \ (lh) \quad (21)$$

Where the specific CO_2 emissions per liter of diesel are represented by SE_{CO_2}, and its value is 2.7 kg/l.
The following is an estimation of the DG's yearly CO_2 emissions:

$$Annual_{CO_2}\_Emissions = \sum_{t=1}^{8760} CO_2(t) \quad (22)$$

3.5 Model of the Bidirectional or Dual Converter with Charger Controller (BDC-CC)

The BDC-CC operates as an inverter (DC to AC) or rectifier (AC to DC), preventing battery overcharge or deep discharge. Its power rating (P_{BDC-CC}) is determined using the following formulas based on mode [87]. If $P_{WT}(t) > P_{Load}(t)$, or $P_{WT}(t) + P_{PV}(t) \gg P_{Load}(t)$, and $E_{\mathrm{Bat}}(\mathrm{t}) < E_{\mathrm{Bat\_max}}$, the converter charges the battery. The BDC-CC size is estimated as follows:

$$P_{BDC-CC}(t) = [P_{WT}(t) - P_{Load}(t)] * \eta_{Conv} \quad (23)$$

- If $P_{WT}(t) < P_{Load}(t)$, or $P_{WT}(t) + P_{PV}(t) > P_{Load}(t)$ and $E_{\mathrm{Bat}}(\mathrm{t}) < E_{\mathrm{Bat\_max}}$, the battery charges. If $E_{\mathrm{Bat}}(\mathrm{t}) = E_{\mathrm{Bat\_max}}$, surplus power flows to the dump load. The BDC-CC size is estimated as follows:

$$P_{BDC-CC}(t) = [P_{PV}(t) - P_{BC}(t)] * \eta_{Conv} \quad (24)$$

- If $P_{WT}(t) + P_{PV}(t) < P_{Load}(t)$ and $E_{\mathrm{Bat}}(\mathrm{t}) > E_{\mathrm{Bat\_min}}$, the battery discharges via the converter to meet the load. The BDC-CC size is estimated as follows:

$$P_{BDC-CC}(t) = [P_{PV}(t) + P_{BD}(t)] * \eta_{Conv} \quad (25)$$

Based on simulation results, the PWM converter rating is determined using the above formulas [99].

4 Energy Management Strategies

Energy management is essential for IHRES sizing and optimization. This study proposes a method for managing energy in a PV/WTs/DG/battery IHRES, aiming to size components optimally to meet load demand within LPSP limits and handle dump energy (E_{Dump}) to reduce COE. The approach evaluates hourly energy balance over the year. **Figure 9** shows the EMS flowcharts for operating modes, which are described as follows:

- **Mode 1**: In this operational mode, the battery bank's energy level at 't+1' matches the energy level of the previous hour, and the system's total net power delivered is zero. While switches S4, S5, and S6 are open, switches S1, S2, and S3 are closed. This mode of operation is depicted clearly in **Fig. 10(a)**. There will be no power outage, and the expected load demand will be met.
- **Mode 2**: In this operational mode, the RE resources first meet the load demand before storing any excess energy generated in the battery bank. This is only applicable if the battery bank's energy levels are within the minimum and maximum range, i.e., ($E_{Bat\_min} \leq E_{Bat}(t) \leq E_{Bat\_max}$). While switches S4 and S5 remain open, switches S1, S2, and S3 are closed. This operational mode is visually depicted in **Fig. 10(b)**. There will be no power outage, and the expected load demand will be fulfilled.
- **Mode 3**: In this operational mode, the energy from the RE resources first satisfies the load demand. If the battery bank's energy level reaches its maximum limit, (if ($E_{Bat}(t) = E_{Bat\_max}$), then the dump load is operated using the extra energy. Where switches S2 and S4 are open, while switches S1, S3, and S5 are closed, as shown in **Fig. 10(c)**. There will be no power outage, and the expected load demand will be met.
- **Mode 4**: In this mode of operation, the battery bank supplies the shortfall in load demand when the energy generated by the RE sources is insufficient This condition is met when. ($E_{Bat}(t) \geq E_{Bat\_max}$). Switches S1, S2, and S3 are closed, while switches S4 and S5 are open, as illustrated in **Fig. 10(d)**. During this mode of operation, the expected demand will be met, and there will be no power outage.
- **Mode 5**: In this mode of operation, there is not enough energy to match the load demand from the battery bank and RE resources. The DG will then be activated to supply the unmet portion of the load if ($E_{Bat}(t) \leq E_{Bat\_min}$). As soon as the RE resources start to generate enough electricity to fulfill the demands of the entire load, the DG stops. Switches S1, S3, and S4 are closed, while switches S2 and S5 are open, as shown in **Fig. 10(e)**. The battery bank remains in its previous state. The expected load demand will be met, and there will be no power outage.
- **Mode 6**: In this mode of operation, there will be a power outage at time 't' because the battery bank's energy level is below the recommended minimum, and the energy supplied by the RE resources is insufficient to meet the required load demand, i.e. $E_{Bat}(t) = E_{Bat\_min}$, but the DG will operate at its maximum capacity as possible as it can. as illustrated in **Fig. 10(f)**.

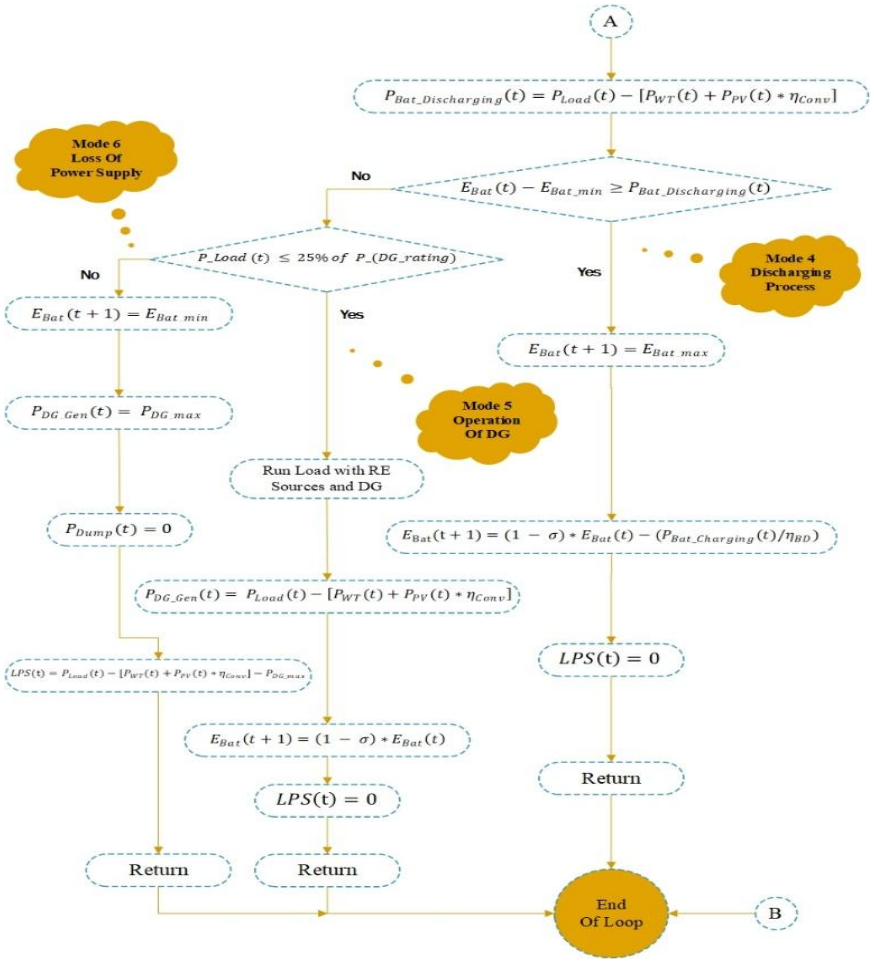

Fig. 9 Flowchart of the EMS operating modes and LPSP acquisition using LF and CC strategies

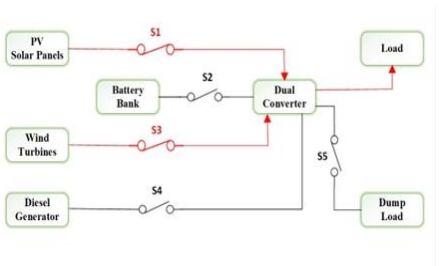

Fig. 10(a)

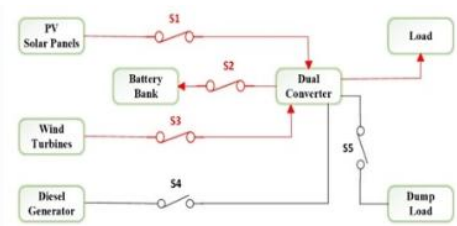

Fig. 10(b)

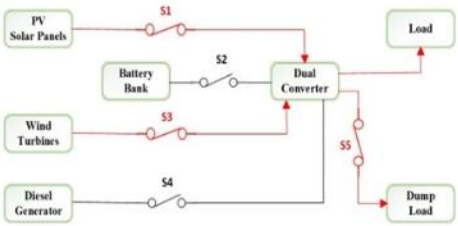

Fig. 10(c)

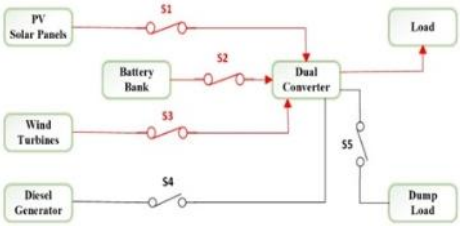

Fig. 10(d)

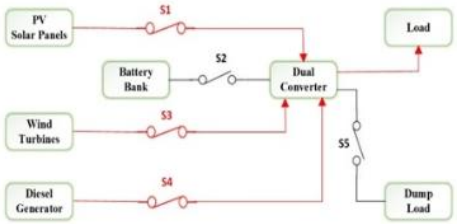

Fig. 10(e)

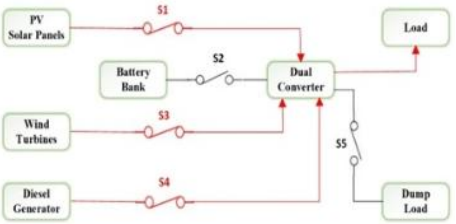

Fig. 10(f)

Fig. 10 Operational modes of the IHRES using LF and CC strategies

5 Optimization

5.1 Economic Assessment of the Off-Grid IHRES

The economic sustainability of the IHRES is evaluated using methods such as net present cost, annual levelized cost, LCC, and payback period. LCC, which reflects the project's total costs over its life cycle, is employed for the economic analysis. This study calculates LCC by summing costs for system components, replacement, erection, capital, O&M, and fuel [100]. COE, a key economic indicator for IHRES, is computed as follows [75]:

$$COE = \frac{LCC * CRF(i,T)}{\sum_{t=1}^{8760} P_{Load}(t)} \tag{26}$$

Where T is the project lifespan (25 years), i is the real net interest rate, and CRF is the capital recovery factor, calculated as follows [59]:

$$CRF(i,T) = \frac{i*(1+i)^T}{(1+i)^T - 1} \tag{27}$$

The discount rate is computed by applying the following formula [79].

$$y = \frac{i_{nom} - f}{1+f} \tag{28}$$

Where i_{nom} is the yearly nominal interest rate (8.25% in this study [101] and f is the yearly inflation rate (4.9% [102]).

The life cycle cost (C_{Life_Cycle}) of the overall project can be estimated by using the following formula:

$$LCC = C_{Initial\_Capital} + C_{O\&M} + C_{Rep} + C_{Fuel} - V_{Scarp} \tag{29}$$

Where $C_{Initial\_Capital}$ is the initial cost, $C_{O\&M}$ is the operation and maintenance cost, C_{Rep} is the replacement cost, C_{Fuel} is the fuel cost, and V_{Scarp} is the scrap value of each IHRES component.

Costs: Installation, civil work, electrical testing, and commissioning are part of $C_{Initial\_Capital}$. Installation and civil works make up 20% of WT system costs and 40% of solar system costs, respectively [100]. $C_{Initial\_Capital}$ can be estimated as follows:

$$C_{Initial\_Capital} = C_{\mathrm{WT}} * P_{R_{WT}} * N_{\mathrm{WT}} + C_{PV} * PV_{panel\_rating} * N_{\mathrm{PV}} + C_{\mathrm{Bat}} * S_{Bat_{rating}} * N_{\mathrm{Bat}} + C_{\mathrm{DG}} * P_{DG\_rating} * N_{\mathrm{DG}} + C_{\mathrm{BDC-CC}} * P_{BDC-CC} \tag{30}$$

Where C_{WT} is the cost of WT with civil works ($/kW), $P_{R_{WT}}$ is the rated WT output power, N_{WT} is the number of WTs, C_{PV} is the cost of PV panels with civil works ($/kW), PV_{panel_rating} is the rated PV power, N_{PV} is the number of PV panels, C_Bat is the cost of batteries ($/kW), $S_{Bat_{rating}}$ is the battery bank rating, N_{Bat} is the number of battery cells, C_{DG} is the DG system cost, P_{DG_rating} is the DG's rated power, and N_{DG} is the number of DGs.

$C_{O\&M}$ values, based on analysis from studies [101-104], are estimated and can be calculated using the following formula [105]:

$$C_{O\&M} = \sum_{j=1}^{T} C_{O\&M}(1) * \left(\frac{1}{(1+i)^j}\right) \tag{31}$$

Where $C_{O\&M}(1)$ is the project's first year operating and maintenance costs. There is another formula which can be expressed as:

$$C_{O\&M} = C_{O\&M\_\mathrm{WT}} * T_{\mathrm{WT}} + C_{O\&M\_\mathrm{PV}} * T_{\mathrm{PV}} + C_{O\&M\_\mathrm{Bat}} * T_{\mathrm{Bat}} + C_{O\&M\_DG} * T_{DG} + C_{O\&M\_BDC-CC} * T_{BDC-CC} \tag{32}$$

Where, $C_{O\&M\_\mathrm{WT}}$, $C_{O\&M\_\mathrm{PV}}$, $C_{O\&M\_\mathrm{Bat}}$, $C_{O\&M\_DG}$, and $C_{O\&M\_BDC-CC}$ are the maintenance and operation costs for WTs, PV panels, battery storage, DGs, and bidirectional converters, respectively. T_{WT}, T_{PV}, T_{Bat}, T_{DG}, and T_{BDC-CC} are their corresponding operating times.

The formula below calculates the present value of the replacement cost of hybrid system components, C_{Rep}, over the system's lifespan [101]:

$$C_{Rep} = \sum_{j=1}^{N_{Rep}} \left[K_{Rep} * C_u * \left(\frac{1}{(1+i)}\right)^{\left(T*\frac{j}{N_{Rep}+1}\right)}\right] \tag{33}$$

Where K_{Rep}, C_u, and N_{Rep} are the replacement component capacity (kw for WTs, PV panels, DGs, and bidirectional converters; kWh for batteries), replacement costs ($/kw for WTs, PV panels, DGs, and bidirectional converters; $/kWh for batteries), and the number of replacements over the project's lifespan TTT, respectively.

The fuel cost of C_{Fuel}, can be calculated from the following formula [103]:

$$C_{Fuel} = \left(\sum_{t=1}^{8760} F_{DG}(t)\right) * P_{Fuel} \tag{34}$$

Where $\sum_{t=1}^{8760} F_{DG}(t)$ is DG's annual fuel consumption (l), and P_{Fuel} is the fuel price assumed to be 0.8 $/l.

The following formula can be used to determine the V_{Scarp} :

$$V_{Scarp} = \sum_{j=1}^{N_{Rep}+1} \left[SV\left(\frac{1}{(1+i)}\right)^{\left(T*\frac{j}{N_{Rep}+1}\right)}\right] \tag{35}$$

Where SV is the scrap value of the project components.

5.2 System Reliability Model

Reliability is defined as the ability of the system to deliver continuous and adequate power to meet load requirements

over time. In this study, the reliability of the IHRES is assessed using $LPSP$, based on outage hours and total demand. $LPSP$ at hour 't' is calculated as follows [106]:

$$LPS(\mathrm{t}) = \frac{P_{Load}(t)}{\eta_{Conv}} - P_{Gen}(t) - [(1-\sigma) * E_{\mathrm{Bat}}(\mathrm{t}+1) - E_{\mathrm{Bat}}(\mathrm{t})] * \eta_{BD} \quad (36)$$

The LPSP is calculated as follows [134]:

$$LPSP = \frac{\sum_{t=1}^{8760} LPS(\mathrm{t})}{\sum_{t=1}^{8760} P_{Load}(t)} \quad (37)$$

5.3 System uncertainty model

This design considers $v_i(t)$, representing wind speed fluctuations over 8760 hours, based on historical data. To address uncertainty, both deterministic and stochastic models are used, with the focus on stochastic uncertainty, where variations are modeled by probability distributions [41].

Probability distributions capture changes in time-dependent parameters for stochastic uncertainty. Discrete samples $\xi(\mu, \sigma)$, with mean (μ) and variance (σ), are selected to represent continuous functions. These samples are assigned $v_i(t)$ values and converted to uncertain factors $\varepsilon(t)$ using the following procedure:

$$\varepsilon(t) = v_i(t) + \xi(\mu, \sigma) \quad (38)$$

The average and standard deviation of wind forecast errors for 'n' occurrences are found in the above equation as follows [84]:

$$\mu = \frac{1}{n}\sum_{i=1}^{n} e_i \quad (39)$$

$$\sigma = \sqrt{\frac{1}{n-1}\sum_{i=1}^{n} (e_i - \mu)^2} \quad (40)$$

5.4 Objective function

The objective function minimizes the system's energy cost, determined by the formula below. Costs depend on key variables like N_{WT}, N_{PV}, N_{Bat}, and DG rating, subject to system constraints. The model is nonlinear, based on the previous techno-economic model, and will be analyzed using a metaheuristic algorithm. The objective function is expressed as follows [99]:

$$min\ COE(N_{WT}, N_{PV}, N_{Bat}) = \sum_{C=WT,PV,BAT,DG,BDC-CC}^{min} (LCC)_c \quad (41)$$

5.4.1 Upper and Lower Bounds

This study assumes PV arrays and WTs are the primary energy sources. When there's excess energy, the battery charges; when there is a deficit, the battery discharges (if charged). Thus, wind, solar PV, and the battery bank are subject to the following constraints [87]:

$$N_{WT\_min} \le N_{WT} \le N_{WT\_max} \quad (42)$$

$$N_{PV\_min} \le N_{PV} \le N_{PV\_max} \quad (43)$$

$$N_{Bat\_min} \le N_{Bat} \le N_{Bat\_max} \quad (44)$$

Where N_{WT}, N_{PV}, and N_{Bat} are the number of WTs, PV panels, and battery cells, respectively.

5.4.2 Battery bank storage system limits

The following limits determine the amount of energy that is stored in the battery bank at any particular time "t" [94]:

$$E_{Bat\_min} \le E_{Bat}(t) \le E_{Bat\_max} \quad (45)$$

Where E_{Bat_max} and E_{Bat_min} are the maximum and minimum battery storage levels, calculated as follows:

$$E_{Bat\_max} = \left(\frac{N_{Bat} \times V_{Bat} \times K_{Bat}}{1000}\right) * SOC_{Bat\_max} \quad (46)$$

$$E_{Bat\_min} = \left(\frac{N_{Bat} \times V_{Bat} \times K_{Bat}}{1000}\right) * SOC_{Bat\_min} \quad (47)$$

Where V_{Bat} and K_{Bat} are the battery voltage and rated capacity (Ah), and SOC_{Bat_min} *and* SOC_{Bat_max} are the minimum and maximum states of charge, calculated as follows [94]:

$$SOC_{Bat\_min} = 1 - DOD \quad (48)$$

$$SOC_{Bat\_max} = SOC_{Bat\_min} - DOD \quad (49)$$

Where DOD is the battery's depth of discharge, and **Fig. 11** shows the relationship between lead-acid battery life cycle and DOD.

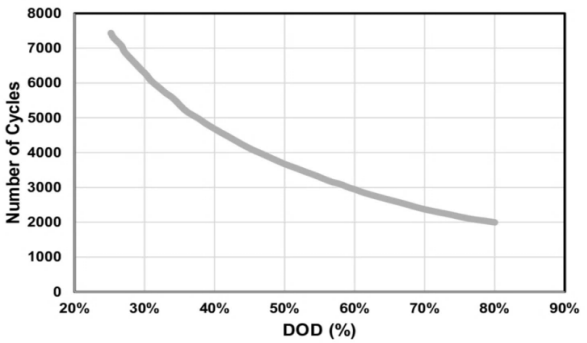

Fig. 11 The typical lifecycle of RS lead acid-SSIG batteries versus DOD

5.4.3 Operating limits of the diesel generator

The DG efficiency improves at higher loads; thus, 25% of its rated capacity is the minimum operating threshold used in this paper. It operates only when the following conditions are satisfied [31]:

$$\frac{P_{Load}(t)}{\eta_{Conv}} \leq 25\%\ of\ P_{DG\_rating} * \Delta t \quad (50)$$

Where $P_{Load}(t)$ is the hourly load, η_{Conv} is the converter efficiency, P_{DG_rating} is DG rated power, and Δt is the simulation time interval.

5.4.4 Loss of power supply and dump energy limits

$LPSP$ and dump energy (E_{Dump}) are key indicators of system reliability. The optimization tracks these values to meet defined limits and minimize COE. In this study, the allowed limits for $LPSP$ and E_{Dump} are set as follows [102]:

$$LPSP \leq 5\%\ of\ ADL \quad (51)$$

$$E_{Dump} \leq 4\%\ of\ ADL \quad (52)$$

Where ADL is the total annual demand load calculated as follows:

$$ADL = \sum_{t=1}^{8760} P_{Load}(t) \quad (53)$$

5.5 The Suggested Algorithm

The study utilizes the Salp Swarm Algorithm (SSA), a metaheuristic method recognized for its ability to identify global optima in complex problems. SSA is inspired by salp swarm behavior, as introduced in [107].

Salps are small, barrel-shaped, jellyfish-like creatures. **Fig. 12(a)** shows their structure, while **Fig. 12(b)** illustrates how they form chains in swarms to search for food.

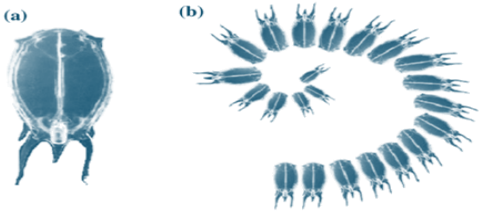

Fig. 12 (a) Salp and (b) Salp Swarm Chain

5.5.1 The Salp swarm algorithm (SSA)

In the mathematical model of the salp chain, the population is divided into two groups: a leader and followers. The leader, located at the front, directs the swarm. Like other swarm-based algorithms, salps are positioned in an n-dimensional search space, where n is the number of objective variables. Their positions are stored in a two-dimensional matrix 'Z', and the swarm aims to reach the food source 'f'. The leader's position is updated as follows [76]:

$$Z_q^1 = \begin{cases} f_q + [c_1 * \left((ul_q - ll_q) * c_2 + ll_q \right)] c_3 \geq 0 \\ f_q - [c_1 * \left((ul_q - ll_q) * c_2 + ll_q \right)]\ c_3 < 0 \end{cases} \quad (54)$$

Where Z_q^1 indicates the position of the leader salp in the q^{th} dimension. The lower and upper bounds of the q^{th} dimension are denoted by ll_q and ul_q. c_1, c_2 and c_3 are random numbers.

The leader modifies its position in response to the food source. Coefficient c_1, shown below, is crucial for balancing exploration and exploitation in SSA.

$$c_1 = 2e^{-\left(\frac{4u}{U}\right)^2} \quad (55)$$

Where u and U are the maximum and current numbers of iterations, respectively.

Random integers c_2 and c_3 are generated in the [0,1] interval, determining the step size and direction (positive or negative) for the next position in the q^{th} dimension. The followers' positions are updated using the following formula based on Newton's law of motion [94]:

$$Z_q^i = \frac{1}{2} a t^2 + V_0 t \quad (56)$$

Where V_0 is the initial speed, t is the time interval, and $i \geq 2$ indicates that Z_q^i is the position of the i^{th} follower salp in the q^{th} dimension and a is the acceleration rate and equals $a = \frac{V_{final}}{t}$ where $V_{final} = \frac{Z - Z_0}{t}$. An iteration is defined as a time 't'; the difference between two iterations is regarded as 1, and if $V_0 = 0$, Z_q^i is defined as follows [105]:

$$Z_q^i = \frac{1}{2} * (Z_q^i + Z_q^{i-1}) \quad (57)$$

Where Z_q^i indicates the position of the i^{th} follower salp in the q^{th} dimension when $i \geq 2$. The salp chains are simulated using the previous formula.

SSA offers benefits like simplicity, ease of implementation, and high efficiency. It rapidly solves optimization problems to find global optimum values. The SSA process for determining the ideal IHRES size with the lowest COE, using the most economical WTs and meeting $LPSP$ and E_{Dump} limits, is detailed. Input data for the program is shown in the flowchart in **Fig. 13**.

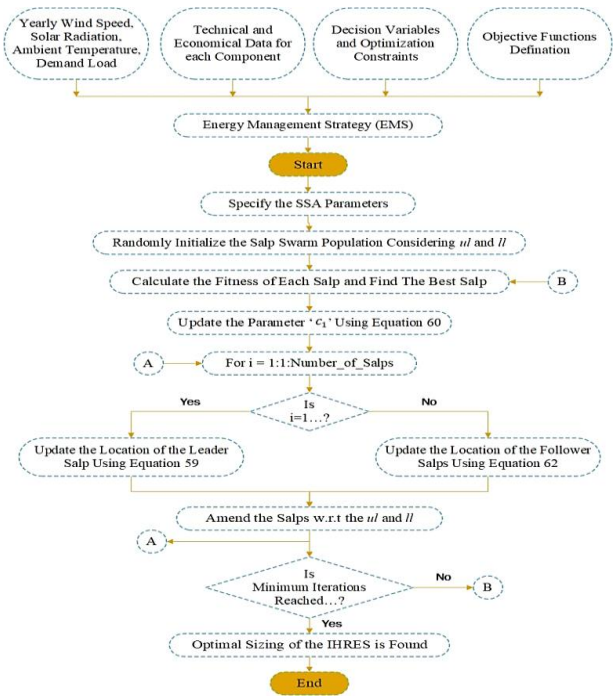

Fig. 13 Flowchart depicting the procedure for determining the optimal IHRES sizing using SSA

6 Results and Discussion

The optimal sizing of an off-grid IHRES was assessed for New Minya City. The site experiences an average wind speed of 5.19 m/s at a height of 10 meters and receives an average daily solar radiation of 6.05 kWh/m²/day. **Table 1** and **Table 2** present the technical specifications of ten wind turbines from various manufacturers, along with the parameters related to the load profile, PV system, battery storage, and diesel generator. The designed system is evaluated over a 25-year operational lifespan.

The simulation results were generated using MATLAB. As previously mentioned, the control parameters and constraints for the optimized variables were established. The sensitivity analysis was conducted on two key computational parameters of the Salp Swarm Algorithm (SSA): the number of search agents (population size) and the number of iterations. The population size varied between 10, 20, 30, and 50 agents, while the number of iterations was evaluated at 50, 100, and 150.

Results showed that increasing the population size led to better convergence and slightly improved the objective function (COE), but with increased computational time. A population size of 30 agents and 100 iterations provided the best trade-off, offering a minimum COE with acceptable computational effort. Further increases beyond 100 iterations resulted in marginal improvement due to convergence saturation.

Table 3 outlines the economic parameters associated with each HRES component. It includes details on $C_{Initial\_Capital}$, $C_{O\&M}$, C_{Rep}, C_{Fuel}, and V_{Scarp}, as well as the expected useful life of the components.

6.1 Optimal combination of system components

This study utilizes the SSA method, implemented in MATLAB, to determine the optimal sizing of a microgrid for a remote site in Egypt's New Minya Governorate. The system configuration includes (i) wind turbines (WTs), (ii) photovoltaic (PV) modules, (iii) battery banks, and (iv) diesel generator (DG) units, all selected to satisfy the site's load requirements.

To reduce dependence on DGs and lower the COE, while ensuring high reliability and performance, a stepwise DSM strategy is applied. This operational approach for the microgrid is illustrated in **Fig. 14**.

Figure 15 illustrates the variation in the Cost of Energy (COE) across different optimization algorithms applied to the WT5 configuration. Among all tested methods, the Salp Swarm Algorithm (SSA) achieved the lowest COE value of 0.21957 $/kWh, outperforming other algorithms such as DA, GRO, ALO, PSO, MFO, and WOA. This superior performance is attributed to SSA's strong global search capability and fast convergence. Notably, WOA resulted in the highest COE value (0.22717 $/kWh), indicating less optimal sizing decisions.

The figure clearly highlights the advantage of SSA in minimizing COE for isolated hybrid renewable systems. **Table 4** provides a detailed quantitative comparison of SSA against seven other metaheuristic algorithms in terms of COE, number of iterations to convergence, and fuel cost. As shown in **Figure 16**, the SSA algorithm converged to the optimal solution after just 53 iterations, demonstrating the fastest performance among all techniques.

While most algorithms converged to acceptable COE values (between 0.220 and 0.227 $/kWh), only SSA achieved the optimal trade-off between low COE, minimal fuel usage, and system reliability. Although its fuel cost was slightly higher due to fewer batteries (leading to more DG usage), SSA still delivered the best overall system economics.

The SSA method outperforms other optimization techniques by reaching the minimum values faster and more effectively. Simulation results confirm that the configuration with the lowest LCC and $LPSP$ within the given constraints achieves the lowest COE. SSA predicts an optimal COE of 0.21975 $/kWh, a life cycle cost (LCC) of 4.5433108 $, and an $LPSP$ of 0.0499-meeting the acceptable limit of $LPSP \leq 0.05$.

The SSA algorithm calculates 78 WTs, 134,946 PV modules, 29,056 battery banks, and 21 DG units to minimize COE at the chosen site. The COE obtained through SSA demonstrates that the hybrid microgrid system can provide cost-effective electricity to the remote town. **Figure 17** and **Figure 18** display the objective function components, including life cycle cost (LCC) and fuel cost, for comparison across optimization methods.

Although SSA provides the lowest COE, it incurs the highest gasoline cost. This is because SSA minimizes the number of battery storage units (29,056), leading to higher initialization and replacement costs. As a result, reducing the number of battery storage units lowers COE. However, if the storage capacity is decreased, the DG operates longer, increasing fuel consumption and raising the annual fuel cost.

6.2 Uncertainty analysis

This study assesses how wind speed and load demand uncertainty affect IHRES performance. Wind speed is predicted using MLE and LSM (These methods were used on historical hourly wind data (8760 hours), ensuring a realistic simulation of wind speed variability across the year) to estimate the Weibull distribution's scale and shape parameters. With these parameters and actual wind data from New Minya, Egypt, a wind speed probability distribution is shown in **Fig. 19**, and a forecast is provided in **Fig. 20**.

The demand load uncertainty is analyzed using a Monte Carlo simulation, where the mean and standard deviation of the load (kW) are computed to form a probability distribution for the actual demand load, as shown in **Fig. 21**. This allows for the expression of the uncertain demand load, as depicted in **Fig. 22**.

Table 1 The technical specifications of the IHRES

Component	WT No.	Manufacturer	P_{R_WT} (kw)	D (m)	u_{cutin} (m/s)	u_{rated} (m/s)	u_{cutoff} (m/s)	H (m)
Wind Turbines	WT 1	Enercon-1	330	34	3	13	34	50
	WT 2	ACSA_1	225	27	3.5	13.5	25	50
	WT 3	Fuhrlander_3	250	50	2.5	15	25	42
	WT 4	Ecotecnia_2	600	44	4	14.5	25	45
	WT 5	ITP-1	250	30	3	12	25	50
	WT 6	NEPC_3	400	31	4	15	25	36
	WT 7	Southern Wind Farms	225	29.8	4	15	25	45
	WT 8	Enercon_2	330	33.4	3	13	34	37
	WT 9	NEPC_2	250	27.6	4	17	25	45
	WT 10	India Wind Power	250	29.7	3	15	25	50

Component	Parameter	Value	Unit
Photovoltaic Panels	Model	JKM400M-72H-V	
	Maxpower	400	Watt
	Length	2008	mm
	Width	1002	mm
	Thickness	40	mm
	Module Efficiency	16.3	%
	Operating Temperature	-10 : 85	^{0}C
	Temperature Coefficient		%

Table 2 The technical specifications of the IHRES

Component	Parameter	Value	Unit
Battery Bank	Model	RS Lead Acid-SSIG 06 490-Battery	
	Nominal Capacity (SBAT)	490	Ah
	Nominal Voltage (VBAT)	6	Volt
	Round Trip Efficiency ($\eta rbat$)	85	%
	DOD	80	%
	Internal Resistance	< 0.005	Ω
	Operating Temperature	-20 : 45	^{0}C
	Self-discharge rate (%/day) (σ)	0.2	%

Component	Parameter	Value	Unit
Diesel Generator	Model	DGK125F	
	Phase	3	Ph
	Rated Output	100	kW
	Frequency	50	Hz
	Power Factor	80	%
	Dry Weight	2990	Kg
	Net Weight	3670	Kg

Table 3 The economic values of the IHRES

Item	WT (kW)	WT Civil Work (kW)	PV (kW)	PV Civil Work (kW)	Battery (kW)	DG (kW)	Dual Converter (kW)
$\mathbf{C_{Initial\_Capital}}$ ($)	1500	300	1150	460	220	350	300
$\mathbf{C_{O\&M}}$ (%)	3	3	1	1	3	3	Null
$\mathbf{C_{Rep}}$ ($)	1200	Null	Null	Null	176	350	270
$\mathbf{V_{Scarp}}$ (%)	20	20	10	20	20	20	10
Salvage Times	2	1	1	1	7	3	3
Lifetime (Year)	20	25	25	25	4	10	10
No. of Replacements	1	0	0	0	6	2	2

Table 4 Comparison between optimization algorithm SSA and other metaheuristic techniques for WT5

Optimization Techniques		WOA	MFO	PSO	ALO	DA	GRO	SSA
Best Objective Function		0.22717	0.22134	0.22083	0.22055	0.22132	0.22009	0.21957
Best Solution	WT	80	79	77	78	79	78	78
	PV	135410	135343	135117	135253	135016	135006	134946
	Battery	29416	29330	29227	29287	29186	29110	29056
	DG	21	21	21	21	21	21	21
Number of Iterations for Optimal Solution		58	64	58	56	72	75	53
TPC ($)		4.6007e8	4.5766e8	4.5657e8	4.5597e8	4.5749e8	4.5502e8	4.5433e8
Dump Load (%)		0.04	0.039	0.04	0.04	0.04	0.039	0.038

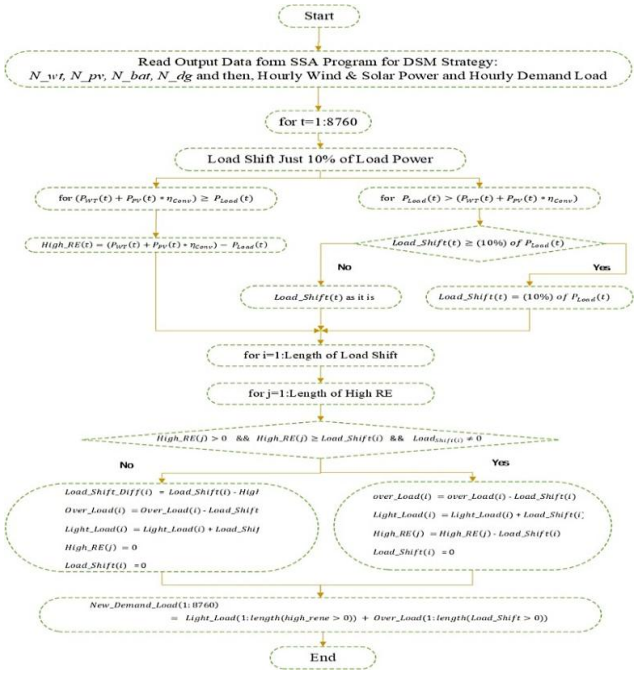

Fig. 14 Flowchart depicting the procedure for applying DSM to the load

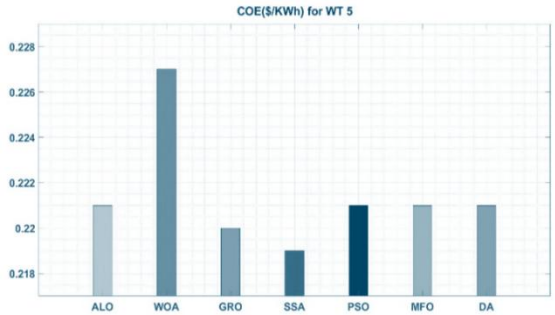

Fig. 15 COE variation across different optimization algorithms

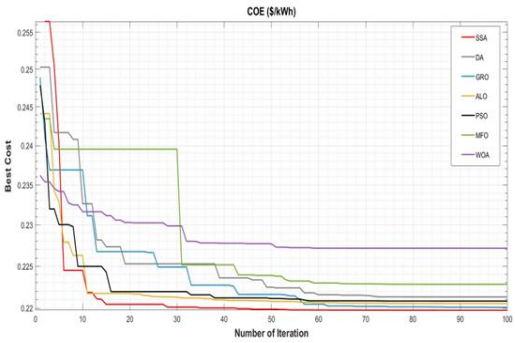

Fig. 16 Convergence curves of optimization techniques

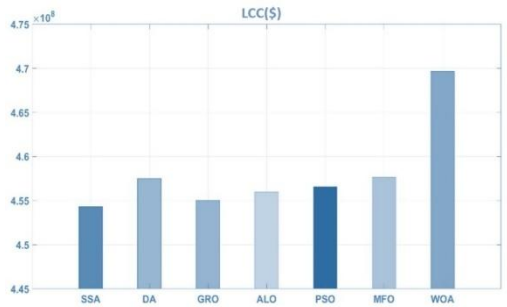

Fig. 17 The life cycle cost ($) of all systems during the project lifetime

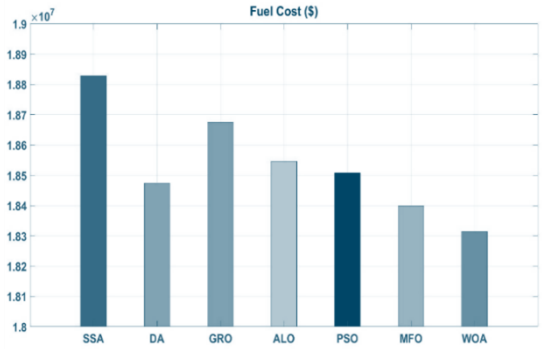

Fig. 18 The fuel cost ($)

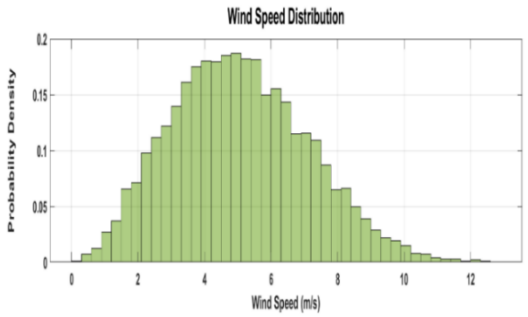

Fig. 19 The probability density of the wind speed distribution

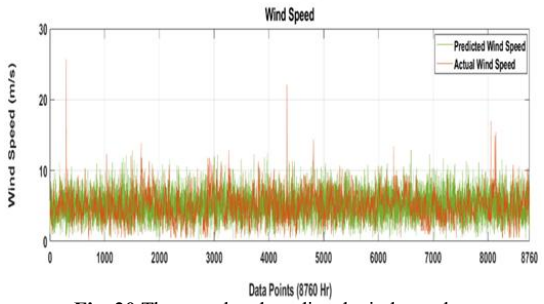

Fig. 20 The actual and predicted wind speed

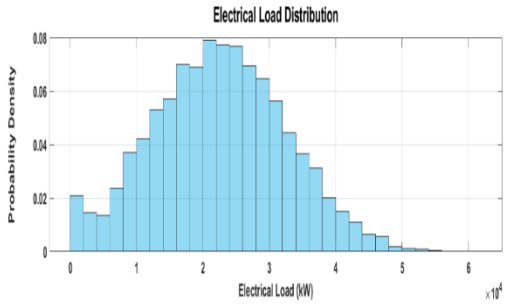

Fig. 21 The probability density of the demand load distribution

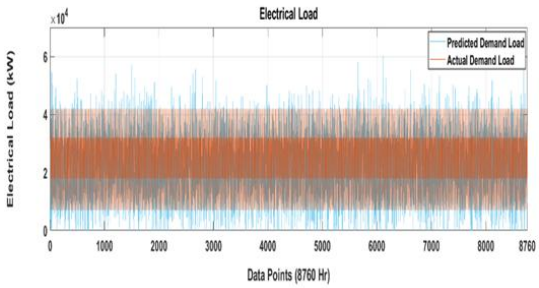

Fig. 22 The actual and predicted demand load

These stochastic models are integrated within the optimization framework to enhance the robustness and reliability of the system design. By incorporating probabilistic variations in key input parameters such as solar irradiance [84], wind speed, load demand, and component availability, the Salp Swarm Algorithm (SSA) is able to effectively capture the inherent uncertainties present in real-world hybrid renewable energy systems. This integration enables the SSA to perform a more comprehensive and adaptive sizing process, ensuring that the resulting system configuration maintains optimal performance under a wide range of possible operational scenarios [41].

Incorporating uncertainties in wind speed and demand load and their impact on key performance indicators such as COE, $LPSP$, and dummy energy, as shown in **Table 5**, affects IHRES constraints ($LPSP$ and dummy energy). For the predicted wind speed (standard deviation: 1.994 m/s, average: 5.087 m/s, RMSE: 2.867 m/s, MAE: 2.265 m/s), the COE decreased from 0.21957 ($/kWh) to 0.2133 ($/kWh), and the $LPSP$ dropped from 5% to 4.43%, with dummy energy increasing three times the optimized value. For the demand load uncertainty (standard deviation: 10231 kW, average: 22583 kW, RMSE: 14251 kW, MAE: 11610 kW), the COE increased from 0.21957 ($/kWh) to 0.2503 ($/kWh), $LPSP$ rose from 5% to 10.28%, and dummy energy grew fivefold.

The next figures illustrate how these uncertainties affect system performance, sizing decisions, and economic outcomes. By visualizing the impact of different uncertainty sources individually and in combination, these figures provide insight into the robustness of the proposed IHRES configuration under variable real-world conditions. This analysis supports the importance of including uncertainty handling within the optimization framework.

6.3 Implementation of the optimal case

Figure 23 illustrates the hourly power variations for the hybrid system under the best SSA scenario. It includes the following: load demand (P_{load}), power from PV panels, WTs, and renewable sources ($P_{WT} + P_{PV}$), net power, battery charging and discharging power ($P_{Bat\_charging}$ & $P_{Bat\_Discharging}$), battery SOC, DG fuel consumption, and operating units, dump load power (P_{Dump}), and LPSP.

Due to low wind speeds, DG units operate at varying power levels to meet energy needs when PV and WT generation is insufficient, and the battery's SOC is low. The dump load absorbs excess power during peak renewable output when the load demand and battery capacity are exceeded.

Figure 24 presents the weekly simulation results over a 168-hour period without applying the DSM technique, showing changes in load power (P_{load}), WT and PV power ($P_{WT} + P_{PV}$), battery charging/discharging ($P_{Bat\_charging}$ & $P_{Bat\_Discharging}$), DG power (P_{DG}), dump load (P_{Dump}), and LPSP. This example highlights two peaks in the daily load curve, helping to explain the optimization algorithm.

The first peak at 1:00 PM is caused by high temperatures, which require air conditioning. The second peak occurs around 6:00 PM, after dusk. At night and early morning, the DG operates continuously due to low renewable energy output. When renewable power exceeds demand, the DG shuts off, and excess energy charges the batteries. $P_{Bat\_Discharging}$, P_{DG}, P_{Dump}, and LPSP will be shown.

Figure 25 shows that applying a 5% load shifting DSM technique reduces the COE from 0.2196 to 0.2191($/kWh). This shift balances energy between deficit and surplus periods, making the load curve more adaptable. The battery storage system's dummy energy reduces reliance on the backup DG, lowering overall system costs.

After applying the DSM, the variations in load power (P_{load}), power from WT and PV systems ($P_{WT} + P_{PV}$), battery charging and discharging ($P_{Bat\_charging}$ & $P_{Bat\_Discharging}$), DG output (P_{DG}), dump load (P_{Dump}), and LPSP will be shown.

In addition, as shown in **Fig. 26**, the simulation results for a particular 168-hour period with the DSM technique for 90% of load shifting in the optimal case, where the COE has decreased from 0.2196 to 0.1989 ($/KWh).

The figures highlight fluctuations in key system parameters: load demand (P_{load}), total WT and PV output ($P_{WT} + P_{PV}$), battery charging/discharging ($P_{Bat\_charging}$ & $P_{Bat\_Discharging}$), DG output (P_{DG}), dump load (P_{Dump}), and LPSP values.

Using the DSM strategy effectively lowers the total system cost, as shown in **Fig. 27**. By aligning demand with available renewable energy, fewer DGs and battery banks are needed, which in turn reduces LPSP and dump energy.

Table 5 Uncertainty analysis results

Uncertainty Aspects	St. Dev	Mean	RMSE	MAE	COE	LPSP	E_{Dummy}
Wind Speed	1.994 (m/s)	5.087 (m/s)	2.867 (m/s)	2.265 (m/s)	0.2133 ($/kwh)	4.43 (%)	1.78 (%)
Demand Load	10231 (kw)	22583 (kw)	14251 (kw)	11610 (kw)	0.2503 ($/kwh)	10.28 (%)	2.01 (%)

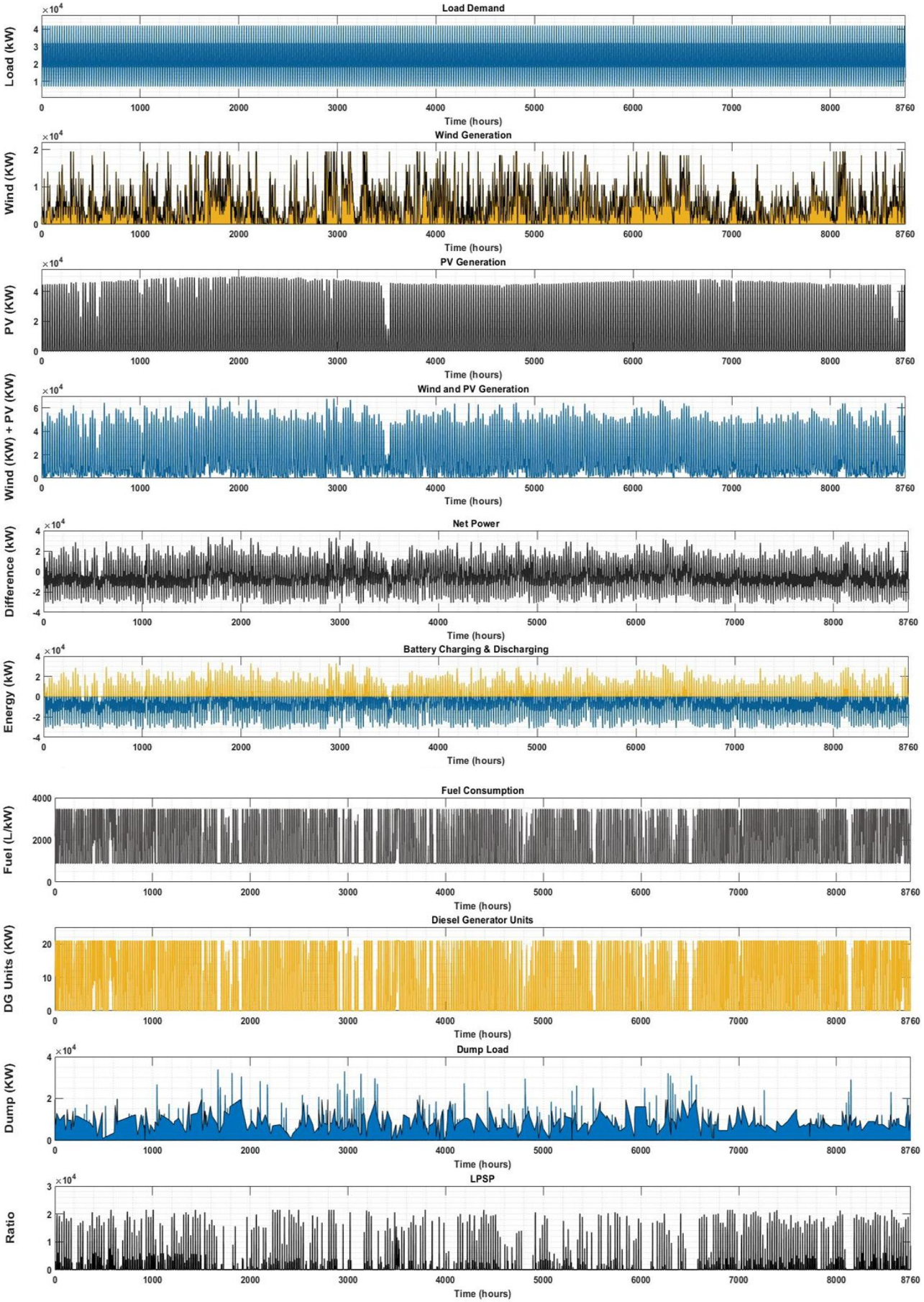

Fig. 23 Simulation results of the optimum solution for 8760 hours (i.e., one year) of operation obtained from SSA

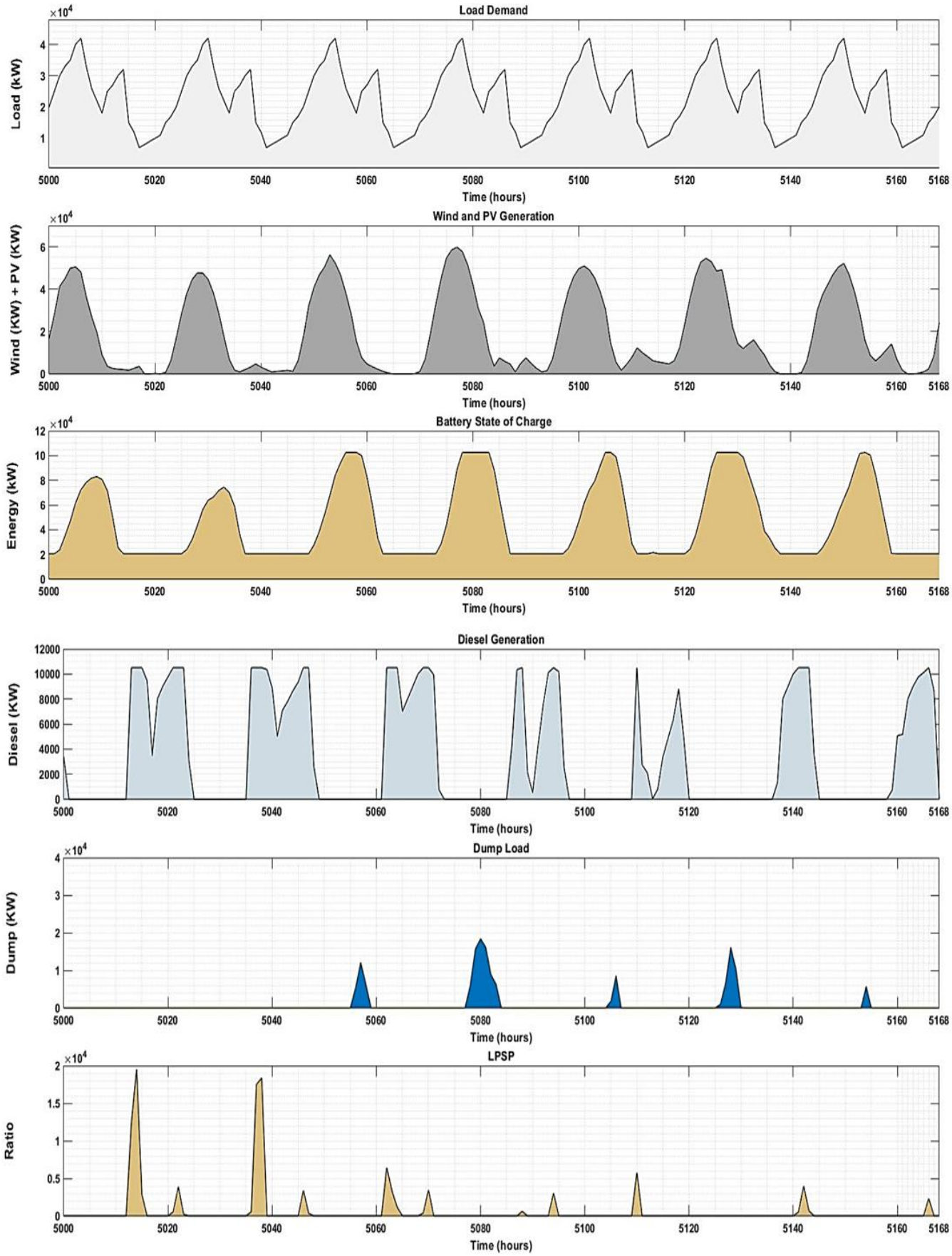

Fig. 24 Simulation results for just one week of operation (168 hours) of the optimum solution derived from SSA without using DSM

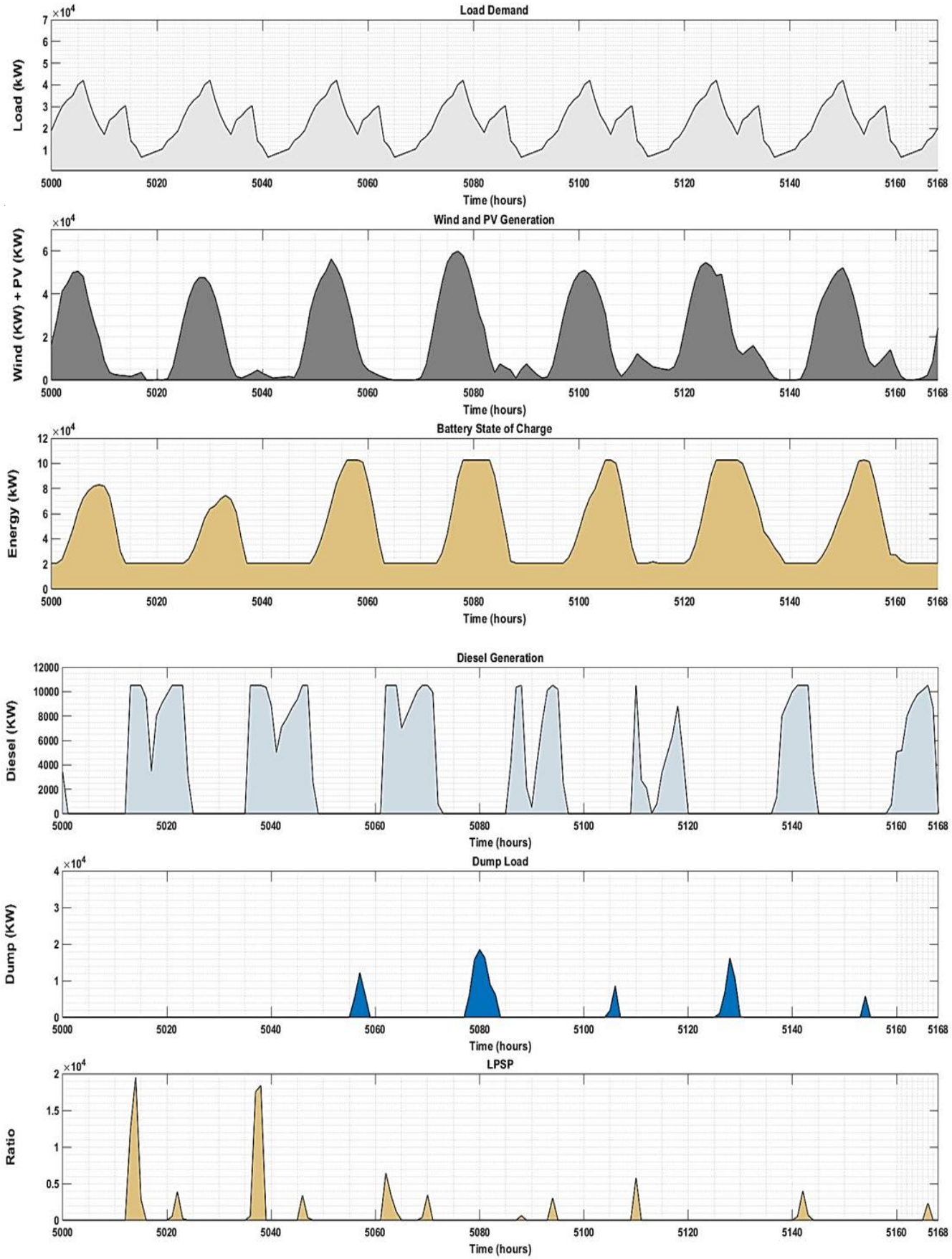

Fig. 25 Simulation results of the optimum possible solution, derived from SSA, using a 5% load-shifting DSM method over a full week of operation (168 hours)

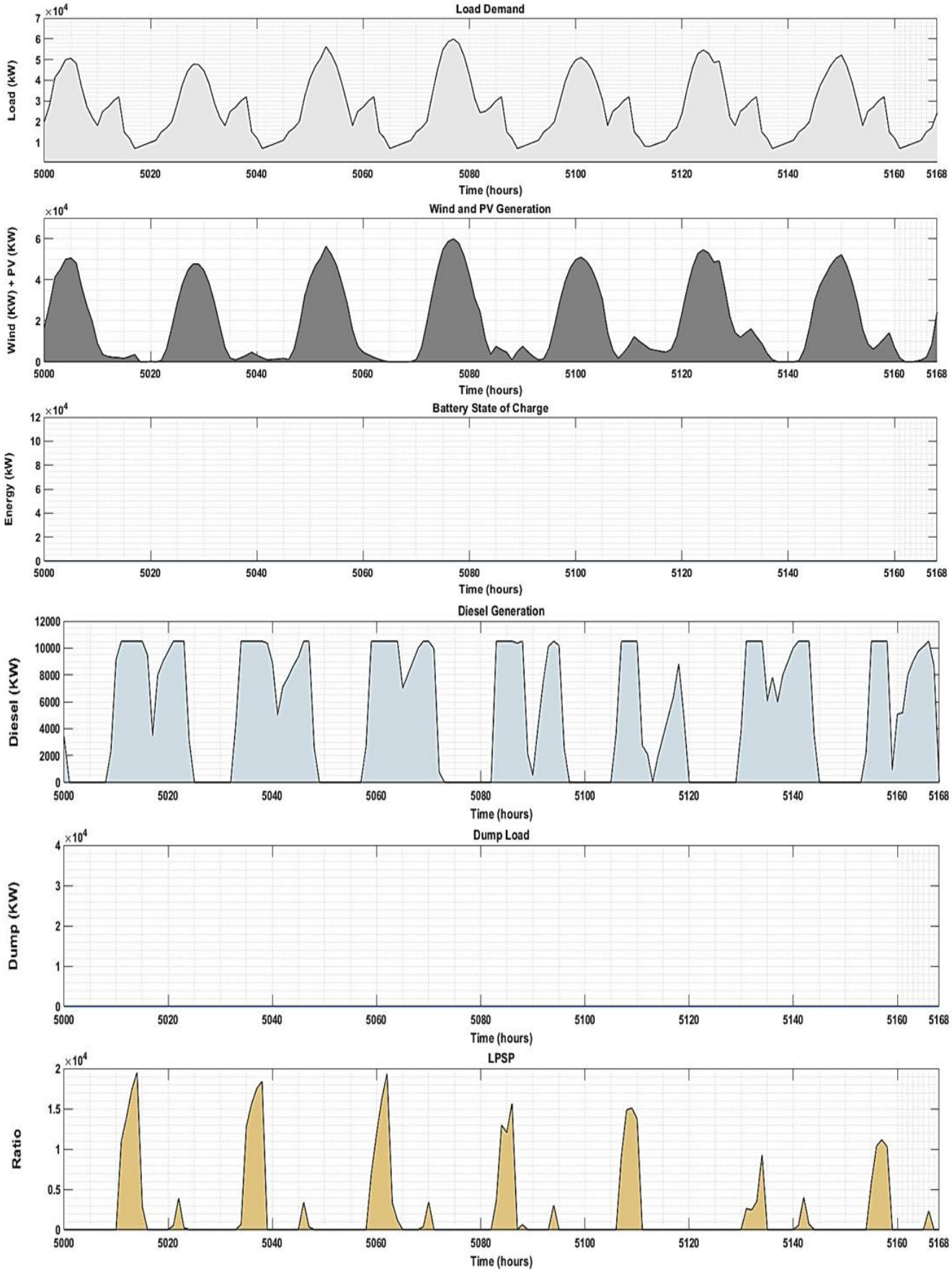

Fig. 26 Simulation results of the optimum possible solution, derived from SSA, using a 90% load-shifting DSM method over a week of operation (168 hours)

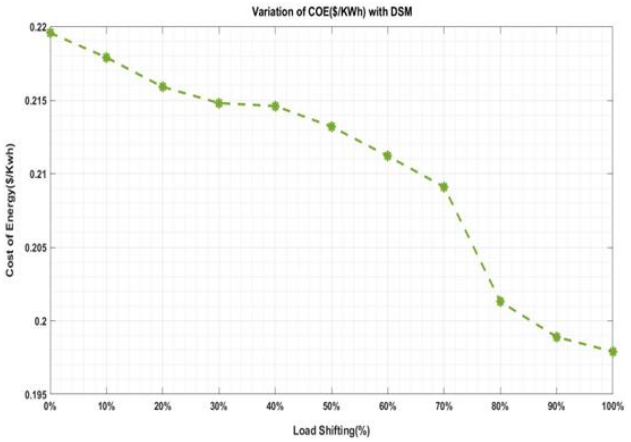

Fig. 27 The COE ($/kWh) with load shifting percentage (%)

7 Conclusion

This paper develops a high-performance program combining multiple metaheuristic algorithms and strategies like LF, CC, and DSM for optimizing hybrid WT/PV/DG/battery bank systems in New Minya city, Egypt. The system design considers uncertainty in natural resources (sun and wind) and economic changes based on real-time weather data. To improve reliability, IHRES units are connected via hybrid DC and AC buses, with a dummy load absorbing surplus power once batteries are fully charged.

Seven metaheuristic optimization methods, including WOA, MFO, PSO, ALO, DA, GRO, and SSA, which are used to determine the optimal configuration for a hybrid renewable energy system. SSA showed the fastest convergence and highest efficiency in reaching the global optimum. This study offers valuable insights for decision-makers in New Minya, Egypt, showing that hybrid systems can lessen reliance on fossil fuels.

This program efficiently estimates the optimal IHRES size, targeting the lowest COE, 5% LPSP, minimal greenhouse gases, and dummy energy at 4% of total demand load, all while ensuring high reliability and performance. The key design parameters include N_WT, N_PV, DG capacity, and battery bank size. The following summarizes these results:

- Presenting high-performance metaheuristic algorithms that outperform traditional deterministic methods and commercial software in solving hybrid RE system design challenges.
- SSA achieves the global optimum with minimal computing resources, delivering the lowest cost. It requires fewer iterations than other methods and demonstrates high efficiency and speed.
- The multi-objective function optimizes the sizing of the hybrid PV, WT, DG, and battery system, reducing dummy energy, COE, and LPSP while enhancing performance and reliability, improving system efficiency.
- Using DSM strategies, the COE dropped from 0.21957 to 0.2159 ($/KWh) with 20% load shifting, LF, CC, and energy conservation techniques. These approaches effectively reduced system component size and LCC while meeting load demand.
- Conducting uncertainty analysis to show the intermittent behavior of solar and wind, and their effect on power generation from WTs and PV panels.

8 Limitations and Future Work

Although this study provides a robust framework for optimizing hybrid renewable energy systems, several limitations should be acknowledged. The following outlines both the main constraints of the current work and potential directions for future research:

8.1 Limitations

1. **Simplified component modeling:** The system components (PV, WT, battery, DG) were modeled using static efficiency and idealized performance assumptions. Real-world conditions like degradation, temperature effects, and nonlinear converter behavior were not fully captured.
2. **Limited DSM modeling:** The demand-side management strategy used in this study is rule-based and assumes full consumer compliance. Real-world DSM effectiveness may vary due to behavioral and infrastructural factors.
3. **Uncertainty handled statistically:** The modeling of uncertainty was based on historical distributions (Weibull, Monte Carlo) and did not include adaptive control or temporal correlation across parameters.
4. **Isolated system scope:** The study is limited to standalone (off-grid) configurations. Hybrid systems operating in grid-connected or microgrid environments introduce different challenges and opportunities.

8.2 Future work

1. **Dynamic component modeling:** Future studies can incorporate temperature-dependent PV performance, battery degradation modeling, and DG fuel efficiency curves for greater realism.
2. **Adaptive forecasting and control:** Integrating short-term forecasting (e.g., via machine learning) and adaptive control algorithms would allow more responsive and robust energy management.
3. **Advanced DSM integration:** Future research may include price-based or incentive-driven DSM strategies, consumer behavior modeling, and automated load shifting systems.
4. **Grid-connected system expansion:** Exploring hybrid system performance in weakly grid-connected or islanded microgrid scenarios can support wider scalability and improve resilience.

References

[1] S. Mansour, M. Alahmadi, P. M. Atkinson, and A. Dewan, "Forecasting of built-up land expansion in a desert urban environment," Remote Sens., vol. 14, no. 9, p. 2037, 2022, https://doi.org/10.3390/rs14092037.

[2] Awuah, Kwasi Gyau Baffour, and Raymond T. Abdulai. "Urban land and development management in a challenged developing world: an overview of new reflections." Land 11, no. 1 (2022): 129, https://doi.org/10.3390/land11010129.

[3] M. E. Gabr, "Land reclamation projects in the Egyptian Western Desert: Management of 1.5 million acres of groundwater irrigation," Water Int., vol. 48, no. 2, pp. 240–258, 2023, https://doi.org/10.1080/02508060.2023.2185745.

[4] Ukoima, Kelvin Nkalo, Okoro Ogbonnaya Inya, Akuru Udochukwu Bola, and Davidson Innocent Ewean. "Technical, economic and environmental assessment and optimization of four hybrid renewable energy models for rural electrification." *Solar compass* 12 (2024): 100087, https://doi.org/10.1016/j.solcom.2024.100087.

[5] Coban, Hasan Huseyin. "A multiscale approach to optimize off-grid hybrid renewable energy systems for sustainable rural electrification: Economic evaluation and design." *Energy Strategy Reviews* 55 (2024): 101527, https://doi.org/10.1016/j.esr.2024.101527.

[6] H. Dibaba, I. Demidov, E. Vanadzina, S. Honkapuro, and A. Pinomaa, "Feasibility of rural electrification and connectivity—A methodology and case study," Appl. Energy, vol. 315, p. 119013, 2022, https://doi.org/10.1016/j.apenergy.2022.119013.

[7] Icaza-Alvarez, Daniel, Pablo Arias Reyes, Francisco Jurado, and Marcos Tostado-Véliz. "Smart strategies for the penetration of 100% renewable energy for the Ecuadorian Amazon region by 2050." *Journal of Cleaner Production* 382 (2023): 135298, https://doi.org/10.1016/j.jclepro.2022.135298.

[8] Elalfy, Dina A., Eid Gouda, Mohamed Fawzi Kotb, Vladimír Bureš, and Bishoy E. Sedhom. "Comprehensive review of energy storage systems technologies, objectives, challenges, and future trends." *Energy Strategy Reviews* 54 (2024): 101482, https://doi.org/10.1016/j.esr.2024.101482.

[9] Ali, Arshad, Magdalena Radulescu, and Daniel Balsalobre-Lorente. "A dynamic relationship between renewable energy consumption, nonrenewable energy consumption, economic growth, and carbon dioxide emissions: Evidence from Asian emerging economies." *Energy & Environment* 34, no. 8 (2023): 3529-3552, https://doi.org/10.1177/0958305X231151684.

[10] Parveen, Shabana, Saleem Khan, Muhammad Abdul Kamal, Muhammad Ali Abbas, Aamir Aijaz Syed, and Simon Grima. "The influence of industrial output, financial development, and renewable and non-renewable energy on environmental degradation in newly industrialized countries." *Sustainability* 15, no. 6 (2023): 4742, https://doi.org/10.3390/su15064742.

[11] R. M. Hannun and A. H. A. Razzaq, "Air pollution resulted from coal, oil and gas firing in thermal power plants and treatment: a review," in IOP Conference Series: Earth and Environmental Science, IOP Publishing, 2022, p. 012008, https://doi.org/10.1088/1755-1315/1002/1/012008.

[12] Y. Majeed et al., "Renewable energy as an alternative source for energy management in agriculture," Energy Reports, vol. 10, pp. 344–359, 2023, https://doi.org/10.1016/j.egyr.2023.06.032.

[13] Wang, Wenlong. "Green energy and resources: advancing green and low-carbon development." *Green Energy and Resources* 1, no. 1 (2023): 100009, https://doi.org/10.1016/j.gerr.2023.100009.

[14] Yusuf, Mohammad, and Hussameldin Ibrahim. "A comprehensive review on recent trends in carbon capture, utilization, and storage techniques." *Journal of Environmental Chemical Engineering* (2023): 111393, https://doi.org/10.1016/j.jece.2023.111393.

[15] W. Wang, L. W. Fan, and P. Zhou, "Evolution of global fossil fuel trade dependencies," Energy, vol. 238, p. 121924, 2022, https://doi.org/10.1016/j.energy.2021.121924.

[16] X. Hu, "RETRACTED: Green economic recovery in Central Asia by utilizing natural resources," 2023, Elsevier, https://doi.org/10.1016/j.resourpol.2023.103582.

[17] Spiru, Paraschiv. "Assessment of renewable energy generated by a hybrid system based on wind, hydro, solar, and biomass sources for decarbonizing the energy sector and achieving a sustainable energy transition." *Energy Reports* 9 (2023): 167-174, https://doi.org/10.1016/j.egyr.2023.04.316.

[18] P. Dechamps, "The IEA World Energy Outlook 2022–a brief analysis and implications," Eur. Energy Clim. J., vol. 11, no. 3, pp. 100–103, 2023, https://doi.org/10.4337/eecj.2023.03.05.

[19] Russo, M. A., D. Carvalho, N. Martins, and A. Monteiro. "Future perspectives for wind and solar electricity production under high-resolution climate change scenarios." *Journal of Cleaner Production* 404 (2023): 136997, https://doi.org/10.1016/j.jclepro.2023.136997.

[20] A. A. Abou El-Ela, R. A. El-Sehiemy, S. M. Allam, A. M. Shaheen, N. A. Nagem, and A. M. Sharaf, "Renewable energy micro-grid interfacing: economic and environmental issues," Electronics, vol. 11, no. 5, p. 815, 2022, https://doi.org/10.3390/electronics11050815.

[21] Billah, Moatasim, Muhammad Yousif, Muhammad Numan, Izhar Us Salam, Syed Ali Abbas Kazmi, and Thamer AH Alghamdi. "Decentralized smart energy management in hybrid microgrids: Evaluating operational modes, resources optimization, and environmental impacts." *IEEE Access* (2023), https://doi.org/10.1109/ACCESS.2023.3343466s.

[22] Zahedibialvaei, Amir, Pavel Trojovský, Maryam Hesari-Shermeh, Ivana Matoušová, Eva Trojovská, and Štěpán Hubálovský. "An enhanced turbulent flow of water-based optimization for optimal power flow of power system integrated wind turbine and solar photovoltaic generators." *Scientific Reports* 13, no. 1 (2023): 14635, https://doi.org/10.1038/s41598-023-41749-3.

[23] MHellqvist, Laura, and Harald Heubaum. "Setting the sun on off-grid solar?: policy lessons from the Bangladesh solar home systems (SHS) programme." *Climate Policy* 23, no. 1 (2023): 88-95, https://doi.org/10.1080/14693062.2022.2056118.

[24] Al-Ghussain, Loiy, Adnan Darwish Ahmad, Ahmad M. Abubaker, Külli Hovi, Muhammed A. Hassan, and Andres Annuk. "Techno-economic feasibility of hybrid PV/wind/battery/thermal storage trigeneration system: Toward 100% energy independency and green hydrogen production." *Energy Reports* 9 (2023): 752-772, https://doi.org/10.1016/j.egyr.2022.12.034.

[25] Khatri, K. A., Krishna Bikram Shah, J. Logeshwaran, and Ashish Shrestha. "Genetic algorithm based techno-economic optimization of an isolated hybrid energy system." *CRF* 8 (2023): 1447-1450, https://doi.org/ 10.21917/ijme.2023.0249.

[26] Almashakbeh, Atef S., Aouda A. Arfoa, and Eyad S. Hrayshat. "Techno-economic evaluation of an off-grid hybrid PV-wind-diesel-battery system with various scenarios of system's renewable energy fraction." *Energy Sources, Part A: Recovery, Utilization, and Environmental Effects* 45, no. 2 (2023): 6162-6185, https://doi.org/10.1080/15567036.2019.1673515.

[27] Lakhina, Upasana, Nasreen Badruddin, Irraivan Elamvazuthi, Ajay Jangra, Truong Hoang Bao Huy, and Josep M. Guerrero. "An Enhanced Multi-Objective Optimizer for Stochastic Generation Optimization in Islanded Renewable Energy Microgrids." *Mathematics* 11, no. 9 (2023): 2079, https://doi.org/10.3390/math11092079s.

[28] Yimen, Nasser, Louis Monkam, Denis Tcheukam-Toko, Bashir Musa, Roger Abang, Lawrence Fon Fombe, Serkan Abbasoglu, and Mustafa Dagbasi. "Optimal design and sensitivity analysis of distributed biomass-based hybrid renewable energy systems for rural electrification: Case study of different photovoltaic/wind/battery-integrated options in Babadam, northern Cameroon." *IET Renewable Power Generation* 16, no. 14 (2022): 2939-2956, https://doi.org/10.1049/rpg2.12266.

[29] Nallolla, Chinna Alluraiah, and Vijayapriya Perumal. "Optimal design of a hybrid off-grid renewable energy system using techno-economic and sensitivity analysis for a rural remote location." *Sustainability* 14, no. 22 (2022): 15393, https://doi.org/10.3390/su142215393.

[30] Li, Zhi, Xiaohua Zhi, Zhanjun Wu, Gao Qian, Ruicheng Jiang, Bingzheng Wang, Rui Huang, and Xiaoli Yu. "Role of different energy storage methods in decarbonizing urban distributed energy systems: A case study of thermal and electricity storage." *Journal of Energy Storage* 73 (2023): 108931, https://doi.org/10.1016/j.est.2023.108931.

[31] M. A. Mohamed, A. M. Eltamaly, A. I. Alolah, and A. Y. Hatata, "A novel framework-based cuckoo search algorithm for sizing and optimization of grid-independent hybrid renewable energy systems," Int. J. green energy, vol. 16, no. 1, pp. 86–100, 2019, https://doi.org/10.1080/15435075.2018.1533837.

[32] Kazem, Hussein A., Miqdam T. Chaichan, Ali HA Al-Waeli, and Aslan Gholami. "A systematic review of solar photovoltaic energy systems design modelling, algorithms, and software." *Energy Sources, Part A: Recovery, Utilization, and Environmental Effects* 44, no. 3 (2022): 6709-6736, https://doi.org/10.1080/15567036.2022.2100517.

[33] Zaro, Fouad, and Noor A. Ayyash. "Design and Management of Hybrid Renewable Energy System using RETscreen Software: A Case Study." *International Journal of Electrical Engineering and Computer Science* 5 (2023): 164-170, https://doi.org/10.37394/232027.2023.5.17.

[34] Oueslati, Hatem, and Salah Ben Mabrouk. "Techno-economic analysis of an on-grid PV/Wind/Battery hybrid power system used for electrifying building." *Energy Sources, Part A: Recovery, Utilization, and Environmental Effects* 45, no. 4 (2023): 9880-9893, https://doi.org/10.1080/15567036.2019.1683097.

[35] Martire, Mattia, Ahmet Fatih Kaya, Nicolò Morselli, Marco Puglia, Giulio Allesina, and Simone Pedrazzi. "Analysis and optimization of a hybrid system for the production and use of green hydrogen as fuel for a commercial boiler." *International Journal of Hydrogen Energy* 56 (2024): 769-779, https://doi.org/10.1016/j.ijhydene.2023.12.223.

[36] Kushwaha, Pawan Kumar, and Chayan Bhattacharjee. "An extensive review of the configurations, modeling, storage technologies, design parameters, sizing methodologies, energy management, system control, and sensitivity analysis aspects of hybrid renewable energy systems." *Electric Power Components and Systems* 51, no. 20 (2023): 2603-2642, https://doi.org/10.1080/15325008.2023.2210556.

[37] Singh, Nagendra, Shekh Kulsum Almas, Ritesh Tirole, Amit Jain, Siddharth Shukla, and Yogendra Kumar. "Analysis of optimum cost and size of the hybrid power generation system using optimization technique." In *2023 IEEE 12th International Conference on Communication Systems and Network Technologies (CSNT)*, pp. 284-291. IEEE, 2023, http://doi.org/10.1109/ICISC.2017.8068591.

[38] S. Sinha and S. S. Chandel, "Review of software tools for hybrid renewable energy systems," Renew. Sustain. energy Rev., vol. 32, pp. 192–205, 2014, https://doi.org/10.1109/CSNT57126.2023.10134720.

[39] Zhang, Guiju, Caiyuan Xiao, and Navid Razmjooy. "Optimal operational strategy of hybrid PV/wind renewable energy system using homer: a case study." *International Journal of Ambient Energy* 43, no. 1 (2022): 3953-3966, https://doi.org/10.1080/01430750.2020.1861087.

[40] Harrou, Fouzi, Bilal Taghezouit, Sofiane Khadraoui, Abdelkader Dairi, Ying Sun, and Amar Hadj Arab. "Ensemble learning techniques-based monitoring charts for fault detection in photovoltaic systems." *Energies* 15, no. 18 (2022): 6716, https://doi.org/10.3390/en15186716.

[41] Tyagi, Shaurya Varendra, and M. K. Singhal. "A comprehensive review of sizing and uncertainty modeling methodologies for the optimal design of hybrid energy systems." *International Journal of Green Energy* 21, no. 7 (2024): 1567-1612, https://doi.org/10.1080/15435075.2023.2253885.

[42] Rashad, Magdi, Alina Żabnieńska-Góra, Les Norman, and Hussam Jouhara. "Analysis of energy demand in a residential building using TRNSYS." *Energy* 254 (2022): 124357, https://doi.org/10.1016/j.energy.2022.124357.

[43] Dezhdar, Ali, Ehsanolah Assareh, Neha Agarwal, Sajjad Keykhah, Mona Aghajari, and Moonyong Lee. "Transient optimization of a new solar-wind multi-generation system for hydrogen production, desalination, clean electricity, heating, cooling, and energy storage using TRNSYS." *Renewable Energy* 208 (2023): 512-537, https://doi.org/10.1016/j.renene.2023.03.019.

[44] Sharma, Sumit, Yog Raj Sood, Ankur Maheshwari, and Pallav. "Modeling and analysis of autonomous hybrid green microgrid system for the electrification of rural area." *Renewable Energy Systems: Modeling, Optimization and Applications* (2022): 167-190, https://doi.org/10.1002/9781119804017.ch7.

[45] De Britto C, John, S. Nagarajan, and R. Senthil Kumar. "Effective design and implementation of hybrid renewable system using convex programming." *International Journal of Green Energy* 20, no. 13 (2023): 1473-1487, https://doi.org/10.1080/15435075.2022.2160634.

[46] Ghanjati, Chaima, and Slim Tnani. "Optimal sizing and energy management of a stand-alone photovoltaic/pumped storage hydropower/battery hybrid system using Genetic Algorithm for reducing cost and increasing reliability." *Energy & Environment* 34, no. 6 (2023): 2186-2203, https://doi.org/10.1177/0958305X221110529.

[47] Hossain, Md Arif, Ashik Ahmed, Shafiqur Rahman Tito, Razzaqul Ahshan, Taiyeb Hasan Sakib, and Sarvar Hussain Nengroo. "Multi-Objective Hybrid Optimization for Optimal Sizing of a Hybrid Renewable Power System for Home Applications." *Energies* 16, no. 1 (2022): 96, https://doi.org/10.3390/en16010096.

[48] Güven, Aykut Fatih, and Mohamed Mahmoud Samy. "Performance analysis of autonomous green energy system based on multi and hybrid metaheuristic optimization approaches." *Energy Conversion and Management* 269 (2022): 116058, https://doi.org/10.1016/j.enconman.2022.116058.

[49] Premadasa, P. N. D., C. M. M. R. S. Silva, D. P. Chandima, and J. P. Karunadasa. "A multi-objective optimization model for sizing an off-grid hybrid energy microgrid with optimal dispatching of a diesel generator." *Journal of Energy Storage* 68 (2023): 107621, https://doi.org/10.1016/j.est.2023.107621.

[50] Koholé, Yemeli Wenceslas, Clint Ameri Wankouo Ngouleu, Fodoup Cyrille Vincelas Fohagui, and Ghislain Tchuen. "Quantitative techno-economic comparison of a

photovoltaic/wind hybrid power system with different energy storage technologies for electrification of three remote areas in Cameroon using Cuckoo search algorithm." *Journal of Energy Storage* 68 (2023): 107783, https://doi.org/10.1016/j.est.2023.107783.

[51] Chen, Yingfeng, Rui Wang, Mengjun Ming, Shi Cheng, Yiping Bao, Wensheng Zhang, and Chi Zhang. "Constraint multi-objective optimal design of hybrid renewable energy system considering load characteristics." *Complex & Intelligent Systems* 8, no. 2 (2022): 803-817, https://doi.org/10.1007/s40747-021-00363-4.

[52] Maleki, Akbar. "Optimization based on modified swarm intelligence techniques for a stand-alone hybrid photovoltaic/diesel/battery system." *Sustainable Energy Technologies and Assessments* 51 (2022): 101856, https://doi.org/10.1016/j.seta.2021.101856.

[53] Dashtdar, Masoud, Aymen Flah, Seyed Mohammad Sadegh Hosseinimoghadam, Ch Rami Reddy, Hossam Kotb, Kareem M. AboRas, Elżbieta Jasińska, and Michał Jasiński. "Solving the environmental/economic dispatch problem using the hybrid FA-GA multi-objective algorithm." *Energy Reports* 8 (2022): 13766-13779, https://doi.org/10.1016/j.egyr.2022.10.054.

[54] Al Anazi, Abeer Abdullah, Abdullah Albaker, Wongchai Anupong, Abdul Rab Asary, Rajabov Sherzod Umurzoqovich, Iskandar Muda, Rosario Mireya Romero-Parra, Reza Alayi, and Laveet Kumar. "Technical, economic, and environmental analysis and comparison of different scenarios for the grid-connected PV power plant." *Sustainability* 14, no. 24 (2022): 16803, https://doi.org/10.3390/su142416803.

[55] Dsouza, Ozwin Dominic, G. Shilpa, and G. Irusapparajan. "Optimized energy management for hybrid renewable energy sources with Hybrid Energy Storage: An SMO-KNN approach." *Journal of Energy Storage* 96 (2024): 112152, https://doi.org/10.1016/j.est.2024.112152.

[56] A. Bouaouda and Y. Sayouti, "Hybrid meta-heuristic algorithms for optimal sizing of hybrid renewable energy system: a review of the state-of-the-art," Arch. Comput. Methods Eng., vol. 29, no. 6, pp. 4049–4083, 2022, https://doi.org/10.1007/s11831-022-09730-x.

[57] Belboul, Zakaria, Belgacem Toual, Abdellah Kouzou, Lakhdar Mokrani, Abderrahman Bensalem, Ralph Kennel, and Mohamed Abdelrahem. "Multiobjective optimization of a hybrid PV/Wind/Battery/Diesel generator system integrated in microgrid: A case study in Djelfa, Algeria." *Energies* 15, no. 10 (2022): 3579, https://doi.org/10.3390/en15103579.

[58] Pires, Arthur Leandro Guerra, Paulo Rotella Junior, Luiz Célio Souza Rocha, Rogério Santana Peruchi, Karel Janda, and Rafael de Carvalho Miranda. "Environmental and financial multi-objective optimization: Hybrid wind-photovoltaic generation with battery energy storage systems." *Journal of Energy Storage* 66 (2023): 107425, https://doi.org/10.1016/j.est.2023.107425.

[59] George, DX Tittu, R. Edwin Raj, Ananth Rajkumar, and M. Carolin Mabel. "Optimal sizing of solar-wind based hybrid energy system using modified dragonfly algorithm for an institution." *Energy Conversion and Management* 283 (2023): 116938, https://doi.org/10.1016/j.enconman.2023.116938.

[60] Sadeghi, Ali, Akbar Maleki, and Siavash Haghighat. "Techno-economic analysis and optimization of a hybrid solar-wind-biomass-battery framework for the electrification of a remote area: a case study." *Energy Conversion and Management: X* 24 (2024): 100732, https://doi.org/10.1016/j.ecmx.2024.100732.

[61] Bayat, Mohammad, Mohammad Ghiasabadi Farahani, Ali Asghar Ghadimi, Marcos Tostado-Veliz, Mohammad Reza Miveh, and Francisco Jurado. "Optimal siting, sizing and setting of droop-controlled DERs in autonomous microgrids: A new paradigm in microgrid planning." *Electric Power Systems Research* 225 (2023): 109850, https://doi.org/10.1016/j.epsr.2023.109850.

[62] Tay, Godfred, Amevi Acakpovi, Patrick Adjei, George K. Aggrey, Robert Sowah, Daniel Kofi, Maxwell Afonope, and Mustapha Sulley. "Optimal sizing and techno-economic analysis of a hybrid solar PV/wind/diesel generator system." In *IOP conference series: earth and environmental science*, vol. 1042, no. 1, p. 012014. IOP Publishing, 2022, http://doi.org/10.1088/1755-1315/1042/1/012014.

[63] Ayan, Sefer, and Hayrettin Toylan. "Size optimization of a stand-alone hybrid photovoltaic/wind/battery renewable energy system using a heuristic optimization algorithm." *International Journal of Energy Research* 46, no. 11 (2022): 14908-14925, https://doi.org/10.1002/er.8192.

[64] Dashtaki, Amir Ali, Seyed Mehdi Hakimi, Arezoo Hasankhani, Ghasem Derakhshani, and Babak Abdi. "Optimal management algorithm of microgrid connected to the distribution network considering renewable energy system uncertainties." *International Journal of Electrical Power & Energy Systems* 145 (2023): 108633, https://doi.org/10.1016/j.ijepes.2022.108633.

[65] Koholé, Yemeli Wenceslas, Fodoup Cyrille Vincelas Fohagui, Clint Ameri Wankouo Ngouleu, and Ghislain Tchuen. "An effective sizing and sensitivity analysis of a hybrid renewable energy system for household, multi-media and rural healthcare centres power supply: a case study of Kaele, Cameroon." *International Journal of Hydrogen Energy* 49 (2024): 1321-1359, https://doi.org/10.1016/j.ijhydene.2023.09.093.

[66] Mahesh, Aeidapu, and Gangireddy Sushnigdha. "Optimal sizing of photovoltaic/wind/battery hybrid renewable energy system including electric vehicles using improved search space reduction algorithm." *Journal of Energy Storage* 56 (2022): 105866, https://doi.org/10.1016/j.est.2022.105866.

[67] Pramodini, N., MM Rajan Singaravel, and N. Niveditha. "Multi objective optimization of PV/wind hybrid renewable energy system for a zero net energy campus." In *2022 3rd International Conference for Emerging Technology (INCET)*, pp. 1-6. IEEE, 2022, https://doi.org/10.1109/INCET54531.2022.9824135.

[68] González-Ramírez, Juan M., Ángel Arcos-Vargas, and Fernando Núñez. "Optimal sizing of hybrid wind-photovoltaic plants: A factorial analysis." *Sustainable Energy Technologies and Assessments* 57 (2023): 103155, https://doi.org/10.1016/j.seta.2023.103155.

[69] Heydari, Azim, Meysam Majidi Nezhad, Farshid Keynia, Afef Fekih, Nasser Shahsavari-Pour, Davide Astiaso Garcia, and Giuseppe Piras. "A combined multi-objective intelligent optimization approach considering techno-economic and reliability factors for hybrid-renewable microgrid systems." *Journal of Cleaner Production* 383 (2023): 135249, https://doi.org/10.1016/j.jclepro.2022.135249.

[70] Alzahrani, Ahmad, Ghulam Hafeez, Sajjad Ali, Sadia Murawwat, Muhammad Iftikhar Khan, Khalid Rehman, and Azher M. Abed. "Multi-objective energy optimization with load and distributed energy source scheduling in the smart power grid." *Sustainability* 15, no. 13 (2023): 9970, http://doi.org/10.3390/su15139970.

[71] Mahmoudi, Sayyed Mostafa, Akbar Maleki, and Dariush Rezaei Ochbelagh. "A novel method based on fuzzy logic to evaluate the storage and backup systems in determining the optimal size of a hybrid renewable energy system." *Journal of Energy Storage* 49 (2022): 104015, https://doi.org/10.1016/j.est.2022.104015.

[72] A. M. Jasim, B. H. Jasim, F.-C. Baiceanu, and B.-C. Neagu, "Optimized sizing of energy management system for off-grid

hybrid solar/wind/battery/biogasifier/diesel microgrid system," Mathematics, vol. 11, no. 5, p. 1248, 2023, https://doi.org/10.3390/math11051248.

[73] Sallam, Mahmoud E., Mahmoud A. Attia, Almoataz Y. Abdelaziz, Mariam A. Sameh, and Ahmed H. Yakout. "Optimal sizing of different energy sources in an isolated hybrid microgrid using turbulent flow water-based optimization algorithm." *IEEE Access* 10 (2022): 61922-61936, http://doi.org/10.1109/ACCESS.2022.3182032.

[74] Jasim, Ali M., Basil H. Jasim, Florin-Constantin Baiceanu, and Bogdan-Constantin Neagu. "Optimized sizing of energy management system for off-grid hybrid solar/wind/battery/biogasifier/diesel microgrid system." *Mathematics* 11, no. 5 (2023): 1248, https://doi.org/10.1016/j.ijhydene.2024.02.004.

[75] M. Kharrich, L. Abualigah, S. Kamel, H. AbdEl-Sattar, and M. Tostado-Véliz, "An Improved Arithmetic Optimization Algorithm for design of a microgrid with energy storage system: Case study of El Kharga Oasis, Egypt," J. Energy Storage, vol. 51, p. 104343, 2022, https://doi.org/10.1016/j.est.2022.104343.

[76] M. Thirunavukkarasu, Y. Sawle, and H. Lala, "A comprehensive review on optimization of hybrid renewable energy systems using various optimization techniques," Renew. Sustain. Energy Rev., vol. 176, p. 113192, 2023, https://doi.org/10.1016/j.rser.2023.113192.

[77] Kumar, Pankaj, Nitai Pal, and Himanshu Sharma. "Optimization and techno-economic analysis of a solar photo-voltaic/biomass/diesel/battery hybrid off-grid power generation system for rural remote electrification in eastern India." *Energy* 247 (2022): 123560, https://doi.org/10.1016/j.energy.2022.123560.

[78] Brumana, Giovanni, Giuseppe Franchini, Elisa Ghirardi, and Antonio Perdichizzi. "Techno-economic optimization of hybrid power generation systems: A renewables community case study." *Energy* 246 (2022): 123427, https://doi.org/10.1016/j.energy.2022.123427.

[79] Bakht, Muhammad Paend, Mohd Norzali Haji Mohd, Usman Ullah Sheikh, and Nuzhat Khan. "Optimal design and performance analysis of hybrid renewable energy system for ensuring uninterrupted power supply during load shedding." *IEEE Access* 12 (2024): 5792-5813, https://doi.org/10.1109/ACCESS.2024.3349594.

[80] Peash, K. M., and Taskin Jamal. "Optimizing Energy Consumption in a University Campus through Demand Side Management Strategies." In *2023 14th International Conference on Computing Communication and Networking Technologies (ICCCNT)*, pp. 1-7. IEEE, 2023, http://doi.org/10.1109/ICCCNT56998.2023.10306990.

[81] M. A. Jirdehi and S. Ahmadi, "The optimal energy management in multiple grids: Impact of interconnections between microgrid–nanogrid on the proposed planning by considering the uncertainty of clean energies," ISA Trans., vol. 131, pp. 323–338, 2022, https://doi.org/10.1016/j.isatra.2022.04.039.

[82] M. M. Kamal, I. Ashraf, and E. Fernandez, "Planning and optimization of microgrid for rural electrification with integration of renewable energy resources," J. Energy Storage, vol. 52, p. 104782, 2022, https://doi.org/10.1016/j.est.2022.104782.

[83] Kermani, Mostafa, Erfan Shirdare, Giuseppe Parise, Massimo Bongiorno, and Luigi Martirano. "A comprehensive technoeconomic solution for demand control in ports: Energy storage systems integration." *IEEE Transactions on Industry Applications* 58, no. 2 (2022): 1592-1601, https://doi.org/10.1109/TIA.2022.3145769.

[84] Bolurian, Amirhossein, Hamidreza Akbari, and Somayeh Mousavi. "Day-ahead optimal scheduling of microgrid with considering demand side management under uncertainty." *Electric Power Systems Research* 209 (2022): 107965, https://doi.org/10.1016/j.epsr.2022.107965.

[85] Onaolapo, A. K., and B. T. Abe. "An extensive assessment of the energy management and design of battery energy storage in renewable energy systems." *WSEAS Transactions on Power Systems* 19, no. 17 (2024): 146-170, https://doi.org/10.37394/232016.2024.19.17.

[86] Enyew, Bimrew Mhari, Ayodeji Olalekan Salau, Baseem Khan, Issaias Gidey Hagos, Haymanot Takele, and Oluwafunso Oluwole Osaloni. "Techno-Economic analysis of distributed generation for power system reliability and loss reduction." *International Journal of Sustainable Energy* 42, no. 1 (2023): 873-888, https://doi.org/10.1080/14786451.2023.2244617.

[87] Abd El-Sattar, Hoda, Salah Kamel, Mohamed H. Hassan, and Francisco Jurado. "An effective optimization strategy for design of standalone hybrid renewable energy systems." *Energy* 260 (2022): 124901, https://doi.org/10.1016/j.energy.2022.124901.

[88] Teimourian, Hanifa, Mahmoud Abubakar, Melih Yildiz, and Amir Teimourian. "A comparative study on wind energy assessment distribution models: A case study on Weibull distribution." *Energies* 15, no. 15 (2022): 5684, https://doi.org/10.3390/en15155684.

[89] Gudmestad, Ove Tobias, and Anja Schnepf. "Design Basis Considerations for the Design of Floating Offshore Wind Turbines." *Sustainable Marine Structures* 5, no. 2 (2023): 26-34, https://doi.org/10.36956/sms.v5i2.913.

[90] Tang, Xiao-Yu, Qinmin Yang, Bernhard Stoevesandt, and Youxian Sun. "Optimization of wind farm layout with optimum coordination of turbine cooperations." *Computers & Industrial Engineering* 164 (2022): 107880, https://doi.org/10.1016/j.cie.2021.107880.

[91] Orynycz, Olga, Paweł Ruchała, Karol Tucki, Andrzej Wasiak, and Máté Zöldy. "A Theoretical Analysis of Meteorological Data as a Road towards Optimizing Wind Energy Generation." *Energies* 17, no. 11 (2024): 2765, https://doi.org/10.3390/en17112765

[92] S. Dawoud, "Techno Economic Evaluation of Hybrid Energy Isolated Micro-Grids for Rural Areas in Four Zones of Egypt," *J. Adv. Eng. Trends*, vol. 41, no. 2, pp. 153–159, 2021.,https://doi.org/10.21608/jaet.2021.39959.1034.

[93] He, J. Y., Q. S. Li, P. W. Chan, and X. D. Zhao. "Assessment of future wind resources under climate change using a multi-model and multi-method ensemble approach." *Applied Energy* 329 (2023): 120290, https://doi.org/10.1016/j.apenergy.2022.120290.

[94] Güven, Aykut Fatih, Nuran Yörükeren, and Mohamed Mahmoud Samy. "Design optimization of a stand-alone green energy system of university campus based on Jaya-Harmony Search and Ant Colony Optimization algorithms approaches." *Energy* 253 (2022): 124089, https://doi.org/10.1016/j.energy.2022.124089.

[95] Bakhtiar, Elaheh Sadeghi, Afshin Naeimi, Ali Behbahaninia, and Gloria Pignatta. "Size Optimization of a Grid-Connected Solar–Wind Hybrid System in Net Zero Energy Buildings: A Case Study." *Environmental Sciences Proceedings* 12, no. 1 (2022): 12, https://doi.org/10.3390/environsciproc2021012012.

[96] Sharma, Pradosh Kumar, D. Arul Kumar, P. William, D. Obulesu, P. Muthu Pandian, Tasneem KH Khan, and G. Manikandan. "Energy storage system based on hybrid wind and photovoltaic technologies." *Measurement: Sensors* 30 (2023): 100915, https://doi.org/10.1016/j.measen.2023.100915.

[97] Modu, Babangida, Md Pauzi Abdullah, Abba Lawan Bukar, Mukhtar Fatihu Hamza, and Mufutau Sanusi Adewolu. "Energy management and capacity planning of photovoltaic-wind-biomass energy system considering hydrogen-battery storage." *Journal of Energy Storage* 73 (2023): 109294, https://doi.org/10.1016/j.est.2023.109294.

[98] Hassan, Qusay, Marek Jaszczur, Imad Saeed Abdulrahman, and Hayder M. Salman. "An economic and technological analysis of hybrid photovoltaic/wind turbine/battery renewable energy system with the highest self-sustainability." *Energy Harvesting and Systems* 10, no. 2 (2023): 247-257, https://doi.org/10.1515/ehs-2022-0030.

[99] A. M. Eltamaly and M. A. Mohamed, "Optimal sizing and designing of hybrid renewable energy systems in smart grid applications," in Advances in renewable energies and power technologies, Elsevier, 2018, pp. 231–313, https://doi.org/10.1016/B978-0-12-813185-5.00011-5.

[100] A. Yamany, M. A. Mohamed, and Y. Mohammed, "Optimal Sizing and Economic Evaluation of Hybrid Photovoltaic/Wind/Battery/Diesel Generation Systems for Autonomous Utilization," J. Adv. Eng. Trends, vol. 43, no. 1, pp. 47–65, 2024, https://doi.org/10.21608/jaet.2022.131727.1147.

[101] Bouchekara, Houssem REH, Yusuf A. Sha'aban, Mohammad S. Shahriar, Saad M. Abdullah, and Makbul A. Ramli. "Sizing of hybrid PV/battery/wind/diesel microgrid system using an improved decomposition multi-objective evolutionary algorithm considering uncertainties and battery degradation." *Sustainability* 15, no. 14 (2023): 11073, https://doi.org/10.3390/su151411073.

[102] Maleki, Akbar, Zahra Eskandar Filabi, and Mohammad Alhuyi Nazari. "Techno-economic analysis and optimization of an off-grid hybrid photovoltaic–diesel–battery system: Effect of solar tracker." *Sustainability* 14, no. 12 (2022): 7296, https://doi.org/10.3390/su14127296.

[103] Anjum, Tahsin, M. A. Parvez Mahmud, Laveet Kumar, Mamdouh El Haj Assad, and M. A. Ehyaei. "Feasibility analysis of hybrid photovoltaic, wind, and fuel cell systems for on–off-grid applications: A case study of housing project in Bangladesh." *Energy Science & Engineering* 12, no. 8 (2024): 3476-3504, https://doi.org/10.1002/ese3.1830.

[104] Tuyet, Nguyen Thi Yen, Tan Minh Phan, and Thang Trung Nguyen. "The combination of energy storage and renewable energies to reach a maximum profit for power systems." *IEEE Access* (2023), https://doi.org/10.1109/ACCESS.2023.3326354.

[105] Ouederni, Ramia, Bechir Bouaziz, and Faouzi Bacha. "Optimization of a Hybrid Renewable Energy System Based on Meta-Heuristic Optimization Algorithms." *International Journal of Advanced Computer Science and Applications (ijacsa)* 15, no. 7 (2024), https://doi.org/10.14569/ijacsa.2024.0150779.

[106] Fan, Jingya, and Xiao Zhou. "Optimization of a hybrid solar/wind/storage system with bio-generator for a household by emerging metaheuristic optimization algorithm." *Journal of Energy Storage* 73 (2023): 108967, https://doi.org/10.1016/j.est.2023.108967.

[107] Yaghoubi, Mokhtar, Mahdiyeh Eslami, Mohammad Noroozi, Hamed Mohammadi, Osman Kamari, and Sivaprakasam Palani. "Modified salp swarm optimization for parameter estimation of solar PV models." *Ieee Access* 10 (2022): 110181-110194., https://doi.org/10.1109/ACCESS.2022.3213746.